

Cosmology with mirror dark matter II: Cosmic Microwave Background and Large Scale Structure

Paolo Ciarcelluti

*Dipartimento di Fisica, Università di L'Aquila, 67010 Coppito AQ, and
INFN, Laboratori Nazionali del Gran Sasso, 67010 Assergi AQ, Italy
E-mail: ciarcelluti@lngs.infn.it*

Abstract

This is the second paper of a series devoted to the study of the cosmological implications of the existence of mirror dark matter. The parallel hidden mirror world has the same microphysics as the observable one and couples the latter only gravitationally. The primordial nucleosynthesis bounds demand that the mirror sector should have a smaller temperature T' than the ordinary one T , and by this reason its evolution can be substantially deviated from the standard cosmology. In this paper we took scalar adiabatic perturbations as the input in a flat Universe, and computed the power spectra for ordinary and mirror CMB and LSS, changing the cosmological parameters, and always comparing with the CDM case. We found differences in both the CMB and LSS power spectra, and we demonstrated that the LSS spectrum is particularly sensitive to the mirror parameters, due to the presence of both the oscillatory features of mirror baryons and the collisional mirror Silk damping. For $x < 0.3$ the mirror baryon-photon decoupling happens before the matter-radiation equality, so that CMB and LSS power spectra in linear regime are equivalent for mirror and CDM cases. For higher x -values the LSS spectra strongly depend on the amount of mirror baryons. Finally, qualitatively comparing with the present observational limits on the CMB and LSS spectra, we show that for $x < 0.3$ the entire dark matter could be made of mirror baryons, while in the case $x \gtrsim 0.3$ the pattern of the LSS power spectrum excludes the possibility of dark matter consisting entirely of mirror baryons, but they could present as admixture (up to $\sim 50\%$) to the conventional CDM.

1 Introduction

For a more general introduction we send the reader to the first paper of this series [1] (hereafter referred to as Paper I), where we studied the linear evolution of adiabatic scalar primordial perturbations. Here we recall the basics of the mirror matter theory and the main results of previous Paper I.

Mirror matter is an ideal stable dark matter candidate. The basic concept is to have a hidden mirror (M) sector of the Universe which has exactly the same particles and interactions of our observable (O) sector.¹ The theory asserts that a discrete symmetry $P(G \leftrightarrow G')$ interchanging corresponding fields of G and G' , so-called mirror parity, guarantees that both particle sectors are described by the same Lagrangians², with all coupling constants (gauge, Yukawa, Higgs) having the same pattern, so that their micro-

¹From now on all fields and quantities of the mirror sector will have an apex to distinguish them from the ones belonging to the observable or ordinary world.

²In the brane world picture, the M sector can be the same O world realized on a parallel brane.

physics is the same³ [3, 4]. Thus, mirror particles are stable exactly as their ordinary counterparts. In addition, two sectors communicate with each other essentially through gravity. Indeed, they could communicate perhaps also via some other messengers⁴ [5], but they are controlled by free parameters, that we can choose small enough to neglect these interactions.

Many people were interested in mirror world over last years, in particular being motivated by the problems of neutrino physics [6], gravitational microlensing [7], gamma ray bursts [8], flavour and CP violation [9] large scale structure of the Universe [10, 11], galaxy formation [12], orthopositronium lifetime [13, 14], dark matter detection experiments [15], anomalous events within the solar system [16, 17, 18], extrasolar planets [19].

Then, if the mirror hypothesis is verified, the Universe contains, besides the particles of the ordinary sector, also their partners in the mirror sector. However, the fact that there are the same particles and interactions in both sectors does not mean that also their cosmological densities are the same. In fact, two sectors could have different initial conditions, and this is exactly what is required in order to avoid a conflict with the Big Bang nucleosynthesis (BBN) bounds on the effective number of extra light neutrino species. In particular, the BBN bounds imply that the M sector has a temperature lower than the O one, with a ratio $x = T'/T < 0.64$ [20]. We remark that the sensitivity of this limit to the factor x is very low, so that also values $x < 0.7$ could be considered. In order to obtain this situation, the following conditions must be satisfied:

A. After the Big Bang the two systems are born with different temperatures, namely the post-inflationary reheating temperature in the M sector is lower than in the visible one, $T'_R < T_R$. This can be naturally achieved in certain models [21].

B. The two systems interact very weakly, so that they do not come into thermal equilibrium with each other after reheating. This condition is automatically fulfilled if the two worlds communicate only via gravity. If there are some other effective couplings between the O and M particles, they have to be properly suppressed.

C. Both systems expand adiabatically, without significant entropy production. If the two sectors have different reheating temperatures, during the expansion of the Universe they evolve independently, their temperatures remain different at later stages, $T' < T$, and the presence of the M sector would not affect primordial nucleosynthesis in the ordinary world.

As shown in previous papers [1, 11, 20], due to the temperature difference between the two sectors, the key epochs for structure formation take place at different redshifts, and in particular they happens in the M sector before than in the O one. We define the two free parameters describing the mirror world as:

$$x = \frac{T'}{T} \lesssim 0.64 \qquad \beta = \frac{\Omega'_b}{\Omega_b} \gtrsim 1, \qquad (1)$$

where the first limit comes from the aforementioned BBN bounds, while the second one from the hypothesis that mirror matter could constitute an important fraction of dark matter in the Universe. This latter assumption is supported by various baryogenesis scenarios with a hidden sector [22], all obtaining a mirror baryonic density at least equal to the ordinary one.

³There is the possibility that the mirror parity could be spontaneously broken and the weak interaction scales $\langle\phi\rangle = v$ and $\langle\phi'\rangle = v'$ could be different, leading to somewhat different particle physics in the mirror sector [2]. In this paper we consider only the case $v = v'$, where the physics is the same in both sectors.

⁴The possible non-gravitational interactions include photon-mirror-photon kinetic mixing, neutrino-mirror-neutrino mass mixing, and Higgs-boson-mirror-Higgs-boson mixing.

Then, in a so-called Mirror Universe (a misleading expression indicating a Universe made of two sectors, ordinary and mirror) the radiation and matter components are expressed in general by

$$\Omega_r = (\Omega_r)_O + (\Omega_r)_M = (\Omega_r)_O(1 + x^4) = 4.2 \times 10^{-5} h^{-2} (1 + x^4), \quad (2)$$

where the additional term x^4 takes into account the temperature difference between two sectors and is very low in view of the bound (1), and

$$\Omega_m = \Omega_b + \Omega'_b + \Omega_{CDM} = \Omega_b(1 + \beta) + \Omega_{CDM}, \quad (3)$$

where Ω'_b is the contribution of mirror baryonic dark matter (MBDM) to the density.

The relevant epochs for structure formation are matter-radiation equality (MRE), matter-radiation decoupling (MRD) and photon-baryon equipartition, respectively represented by the redshifts:

$$1 + z_{\text{eq}} = \frac{\Omega_m}{\Omega_r} \approx 2.4 \cdot 10^4 \frac{\Omega_m h^2}{1 + x^4}, \quad (4)$$

$$1 + z'_{\text{dec}} \simeq x^{-1}(1 + z_{\text{dec}}) \simeq 1.1 \cdot 10^3 x^{-1}, \quad (5)$$

$$1 + z'_{\text{b}\gamma} = \frac{\Omega'_b}{\Omega'_\gamma} \simeq \frac{\Omega_b \beta}{\Omega_\gamma x^4} = (1 + z_{\text{b}\gamma}) \frac{\beta}{x^4} > 1 + z_{\text{b}\gamma}. \quad (6)$$

Eq. (4) means that the MRE in a Mirror Universe occurs always later than in an ordinary one, while from eqs. (5) and (6) we know that decoupling and equipartition in the M sector happen before than in the O one. If we plot the redshifts of MRE and mirror MRD as functions of x , as in fig. 1 of ref. [1], we obtain their intersection for a value x_{eq} expressed by

$$x_{\text{eq}} \approx 0.046(\Omega_m h^2)^{-1}. \quad (7)$$

This means that for values $x < x_{\text{eq}}$ the mirror decoupling occurs in the radiation dominated period, with consequences on the structure formation process (see Paper I [1] and refs. [10, 11, 20]). Using the value $\Omega_m h^2 = 0.135$, appeared in a recent WMAP fit [23], we obtain the typical value $x_{\text{eq}} \approx 0.34$.

This quantity has a key role in structure formation with mirror dark matter. In fact we know from the results of Paper I [1] and refs. [10, 11]) that for values $x < x_{\text{eq}}$ the evolution of primordial perturbations in the linear regime is practically identical to the standard CDM case. In the same paper we studied the relevant scales for structure formation, finding some interesting results: 1) the mirror Jeans mass M'_J is always smaller than the ordinary one, thus making easier the growth of perturbations; 2) there exist the dissipative mirror Silk scale M'_S (analogous to the Silk scale for ordinary baryons), that for $x \sim x_{\text{eq}}$ has the value of a typical galaxy mass; 3) for $x < x_{\text{eq}}$ we obtain $M'_J \sim M'_S$, so that all the primordial perturbations with masses greater than the mirror Silk mass can grow uninterruptedly.

In the last decade the study of the the Cosmic Microwave Background (CMB) and the Large Scale Structure (LSS) is providing a great amount of observational data, and their continuous improvement provides powerful cosmological instruments that could help us to understand the nature of the dark matter of the Universe. In this context, the analysis of the CMB and LSS power spectra for a mirror baryonic dark matter scenario plays a key role as a cosmological test of the mirror theory. This is exactly the aim of this paper, in which we computed these spectra for a large range of parameters, qualitatively studied the consistence with present observational data, and obtained new useful limits on the

mirror parameter space, broadening our previous studies [11] with many new models and a detailed analysis of their dependence on all the cosmological parameters.

The plan of the paper is as follows. In next section we briefly describe the computed mirror models and the procedure used to obtain the CMB and LSS spectra. In sections 3 and 4 we show respectively the CMB and LSS power spectra for a MBDM scenario, and study their dependence on the mirror parameters, comparing with the CDM case. In addition, we computed the spectrum of mirror CMB photons, comparing it with the analogous for the ordinary sector, and we extended the LSS spectra also to smaller non linear scales. Section 5 analyzes the dependence and the sensitivity of the CMB and LSS power spectra on the cosmological parameters; here we study different mirror models changing one parameter each time. Section 6 is devoted to the comparison of mirror power spectra with current observations, that allows us to obtain some bound on the mirror parameter space. Finally, our main conclusions are summarized in section 7.

2 The mirror models

We computed many models for Mirror Universe, assuming adiabatic scalar primordial perturbations, a flat space-time geometry, and different mixtures of ordinary and mirror baryons, photons and massless neutrinos, cold dark matter, and cosmological constant.

We used the evolutionary equations in synchronous gauge⁵ described in ref. [24]. Since we are working in the Fourier space k , all the \mathbf{k} modes (where \mathbf{k} is the comoving wavevector and k its magnitude) in the linearized Einstein, Boltzmann, and fluid equations evolve independently; thus the equations can be solved for one value of \mathbf{k} at a time. Moreover, all modes with the same k obey the same evolutionary equations.

In the same paper, the Boltzmann equations for massless neutrinos and photons have been transformed into an infinite hierarchy of moment equations F_l that must be truncated at some maximum multipole order l_{\max} . Following the suggestions of authors, an improved truncation scheme⁶ is based on extrapolating the behaviour of F_l to $l = l_{\max} + 1$ as

$$F_{(l_{\max}+1)} \approx \frac{(2l_{\max} + 1)}{k\tau} F_{l_{\max}} - F_{(l_{\max}-1)}, \quad (8)$$

where τ is the conformal time. However, time-variations of the potentials during the radiation-dominated era make even equation (8) a poor approximation if l_{\max} is chosen too small. Thus, in order to obtain a relative accuracy better than 10^{-3} in our final results, in the computation of the potential and the density fields the photons and the massless neutrinos phase space distributions for both the ordinary and mirror sectors were expanded in Legendre series truncating the Boltzmann hierarchies at $l_{\max} = 2000$, using the truncation schemes given by the above expression (8) for massless neutrinos and equations (65) of ref. [24] for photons.

We integrated in this way the equations of motion numerically over the range $-5.0 \leq \log k \leq -0.5$ (where k is measured in Mpc^{-1}) using points evenly spaced with an interval of $\Delta \log k = 0.01$. For purposes of computing the LSS power spectra for larger (non linear)

⁵The difference in the use of other gauges is limited to the gauge-dependent behaviour of the density fluctuations on scales larger than the horizon. The fluctuations can appear as growing modes in one coordinate system and as constant mode in another, as shown in ref. [24] for the synchronous and the conformal Newtonian gauges.

⁶One simple method is to set $F_l = 0$ for $l > l_{\max}$, but it is inaccurate. The authors affirmed that the problem with this scheme is the coupling of multipoles in equations, that leads to the propagation of errors from l_{\max} to smaller l . These errors can propagate to $l = 0$ in a time $\tau \approx l_{\max}/k$ and then reflect back to increasing l , leading to amplification of errors in the interval $0 \leq l \leq l_{\max}$ [24].

scales (see § 4.1) we extended the integration of some models as far as $\log k = 1.0$. All the integrations were carried to the redshift $z = 0$.

The numerical computations were made using a Fortran code that solves the cited equations. We took a pre-existent program written for a standard Universe, made only of the ordinary sector, and then we modified the code in order to simulate a Mirror Universe, which has a second sector. This required to modify and add several subroutines to the code. In fact we are dealing now with two self-interacting sectors, and thus all the equations governing the evolution of the considered components, relativistic (photons and massless neutrinos) and non relativistic (baryons), must be doubled. The cold dark matter equations were not doubled because they have the same physical effects independently of the sector. In addition, the two sectors communicate via gravity, so that they are coupled and influence each other through this interaction. Therefore, there are more regimes than in the standard case, because now they are made up of the couplings between the different ordinary and mirror regimes, the latter being time-shifted from the former according to the laws exposed in previous section.

At last, we normalized our results to the COBE data, following the procedure described by Bunn and White in 1997 [25].

Parameter	min. value	max. value
Ω_m	0.1	0.5
ω_b	0.010	0.030
ω'_b	0.0	$\omega_m - \omega_b$
x	0.1	0.7
h	0.5	0.9
n	0.90	1.10

Table 1: Parameters and their ranges used in mirror models. The values are not evenly spaced, but arbitrarily chosen in the parameter space. Not listed there are the total and vacuum densities, which, being flat models, are $\Omega_0 = 1$ and $\Omega_\Lambda = 1 - \Omega_m$.

For the mirror models, we considered different values of the cosmological parameters, where we add to the usual ones two new mirror parameters: the ratio of the temperatures in the two sectors $x = T'/T$ and the mirror baryons density $\Omega'_b = \beta\Omega_b$ (also expressed via the ratio β of the baryonic densities in the two sectors). Starting from an ordinary reference model, we study the influence of the mirror sector varying the two parameters that describe it for a given ordinary sector, replacing a fraction of CDM (or the entire dark matter) with MBDM. Furthermore, we evaluate the influence of the cosmological parameters for a mirror baryonic dark matter scenario, changing all of them. The values used for the parameters are not on a regular grid, but arbitrarily chosen for the only purpose to better understand the CMB and LSS for a Mirror Universe. At present we are not able to make a grid thin enough to perform a fit of all free parameters (even if we fix some of them) for two reasons: first, we have two further parameters, which lengthen a lot the computational time (by a factor order 10^2), and second our program is much slower than the ones commonly used for a standard Universe, because our models are more complicated in terms of calculus and for our choice to privilege precision instead of performance (at least at this stage⁷). We list the parameters used and their ranges in

⁷The aim of this paper is not a fit of the parameters, but a study of some cosmological observables in a MBDM scenario, and possibly a qualitative test of the mirror theory. After this work, a future step could be just to write a new program much faster than the one here used, which should allow us to fit the parameters and compare the results with other cosmological models.

table 1; the total and vacuum densities (not listed in the table) are fixed by our choice of a flat geometry: $\Omega_0 = 1$ and $\Omega_\Lambda = 1 - \Omega_m$. In addition, in order to study the parameter dependence, we computed models also for different numbers of extra-neutrino species ($\Delta N_\nu = 0.5, 1.0, 1.5$).

3 The cosmic microwave background for a Mirror Universe

As anticipated when we studied the structure formation in Paper I [1] (and predicted or shown in refs. [10, 11, 20]), we expect that the existence of a mirror sector influences the cosmic microwave background radiation observable today; in this section we want to evaluate this effect.

We choose a starting standard model and add a mirror sector simply removing cold dark matter and adding mirror baryons. The values of the parameters for this reference model are: $\Omega_0 = 1$, $\Omega_m = 0.30$, $\Omega_\Lambda = 0.70$, $\omega_b = \Omega_b h^2 = 0.02$, $n = 1.00$, $h = 0.70$, with only cold dark matter (no massive neutrinos) and scalar adiabatic perturbations (with spectral index n). This reference model is not the result of a fit, but is arbitrarily chosen consistent with the current knowledge of the cosmological parameters; however, this is not a shortcoming, because here we want only to put in evidence the differences from a representative reference model (without comparison with observations), and this is a good model for this intention.

From this starting point, first of all we substitute all the cold dark matter with mirror baryonic dark matter (MBDM) and evaluate the CMB angular power spectrum varying x from 0.3 to 0.7 (around the upper limit set by the BBN bounds). This is shown in top panel of figure 1, where mirror models are plotted together with the reference model. The first evidence is that the deviation from the standard model is not linear in x : it grows more for bigger x and for $x \lesssim 0.3$ the power spectra are practically coincident. This is important, because it means that a Universe where all the dark matter is made of mirror baryons could be indistinguishable from a CDM model if we analyze the CMB only. We see the greatest separation from the reference model for $x = 0.7$, but it will increase for hypothetical larger values of x . The height of the first acoustic peak grows for $x \gtrsim 0.3$, while the position remains nearly constant. For the second peak the opposite occurs, i.e. the height remains practically constant, while the position shifts toward higher multipoles l ; for the third peak, instead, we have a shift both in height and position (the absolute shifts are similar to the ones for the first two peaks, but the height now decreases instead of increasing). Observing also other peaks, we recognize a general pattern: except for the first one, odd peaks change both height and location, even ones change location only.

In bottom panel of figure 1 we show the intermediate case of a mixture of CDM and MBDM. We consider $x = 0.7$, a high value which permits us to see well the differences changing ω'_b from ω_b to $4\omega_b$. The dependence on the amount of mirror baryons is lower than on the ratio of temperatures x . In fact, the position of the first peak is nearly stable for all mirror models (except for a very low increase of height for growing ω'_b), while differences appear for other peaks. In the second peak the position is shifted as in the case without CDM independently of ω'_b , while the height is inversely proportional to ω'_b with a separation appreciable for $\omega'_b \lesssim 3\omega_b$. For the third peak the behaviour is the same as for the case without CDM, with a slightly stronger dependence on ω'_b , while for the other peaks there is a weaker dependence on ω'_b . A common feature is that the heights of the peaks are not linearly dependent on the mirror baryonic density, while their positions are practically insensitive to ω'_b but depend only on x .

We will analyze in more detail the x and ω'_b dependence of the peaks, together with other parameters, in § 5.

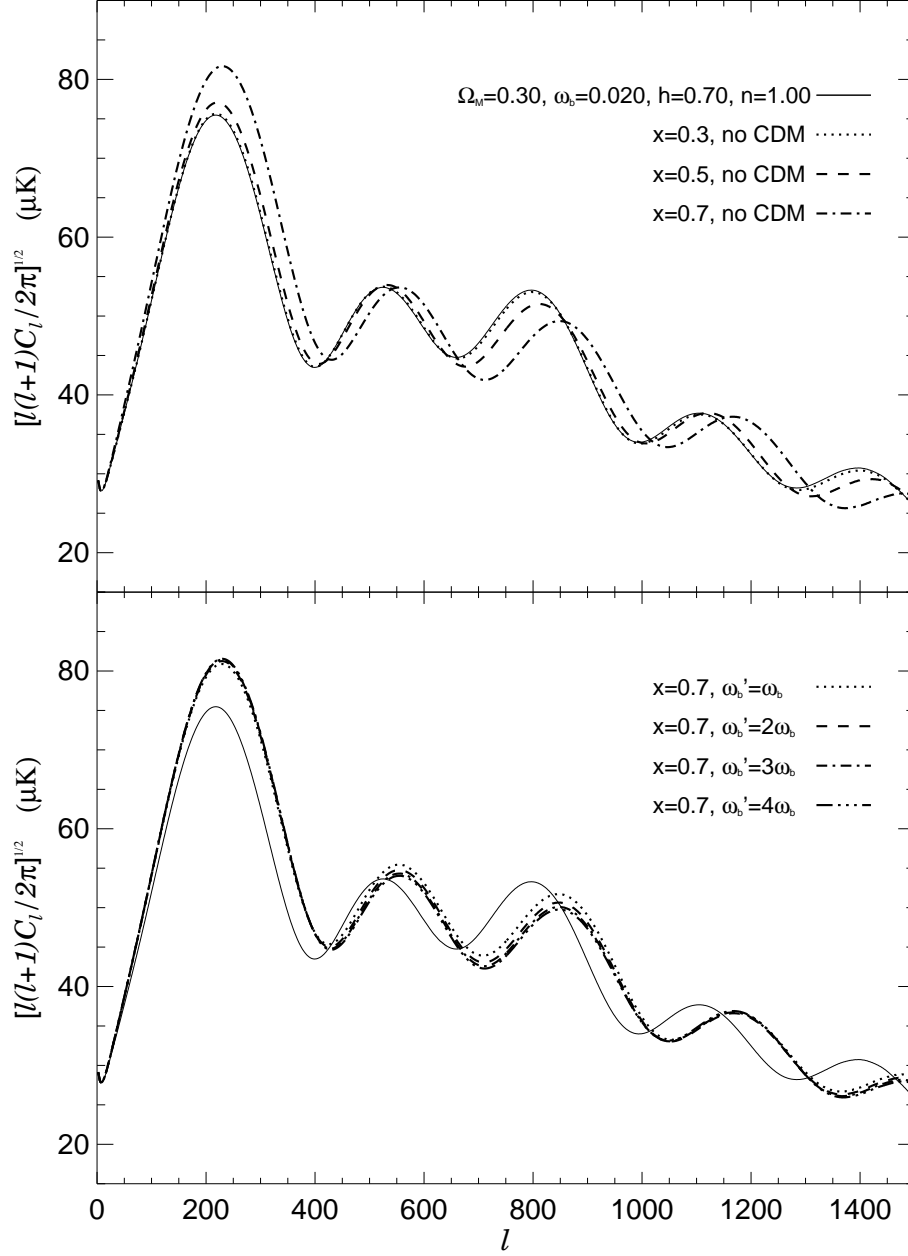


Figure 1: CMB angular power spectrum for different values of x and $\omega'_b = \Omega'_b h^2$, compared with a standard model (solid line). *Top panel.* Mirror models with the same parameters as the ordinary one, and with $x = 0.3, 0.5, 0.7$, and $\omega'_b = \Omega_m h^2 - \omega_b$ (no CDM) for all models. *Bottom panel.* Mirror models with the same parameters as the ordinary one, and with $x = 0.7$ and $\omega'_b = \omega_b, 2\omega_b, 3\omega_b, 4\omega_b$.

3.1 The mirror cosmic microwave background radiation

In the same way as ordinary photons at decoupling from baryons formed the CMB we observe today, also mirror photons at their decoupling formed a mirror cosmic microwave background radiation, which, unfortunately, we cannot observe because they don't couple with the ordinary baryons of which we are made⁸ (instead, it would be possible for an hypothetical mirror observer⁹). Nevertheless, its study is not only speculative, since it is a way to better understand the cosmology with MBDM and our observable CMB.

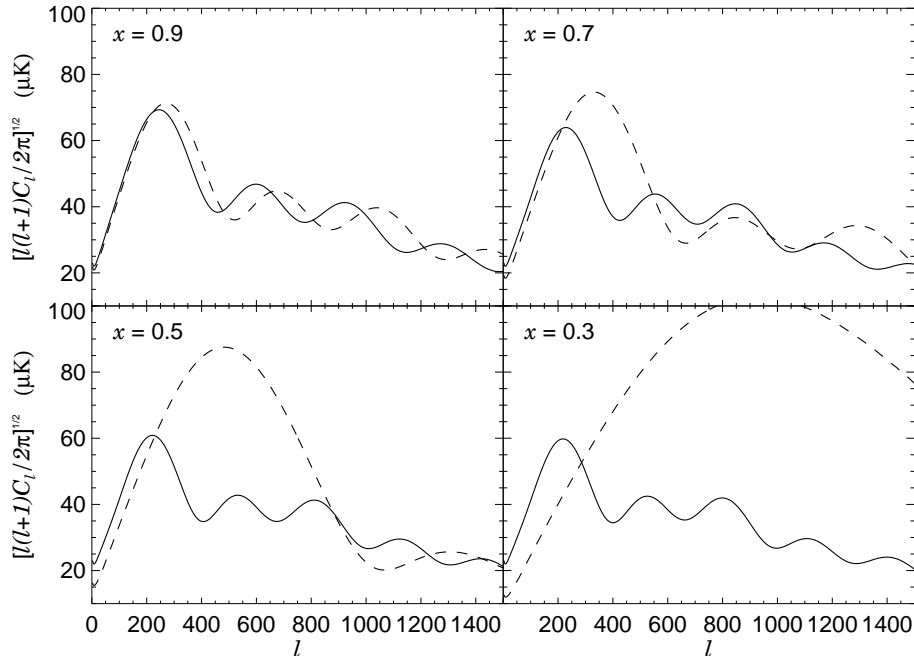


Figure 2: Angular power spectra for ordinary (solid line) and mirror (dashed line) CMB photons. The models have $\Omega_0 = 1$, $\Omega_m = 0.3$, $\omega_b = \omega'_b = 0.02$, $h = 0.7$, $n = 1.0$, and $x = 0.9$ (top-left panel), $x = 0.7$ (top-right panel), $x = 0.5$ (bottom-left panel), $x = 0.3$ (bottom-right panel).

We computed four models of mirror CMB, in order to have enough elements to compare with the corresponding observable CMBs. The chosen parameter values are those usually taken, and the amount of mirror baryons is the same as the ordinary ones, while x is taken as 0.9, 0.7, 0.5 or 0.3 in order to explore different scenarios. Thus the parameters of the models are: $\Omega_0 = 1$, $\Omega_m = 0.3$, $\omega_b = \omega'_b = 0.02$, $x = 0.7$ or 0.5, $h = 0.7$, $n = 1.0$. In figure 2 we plot the ordinary and mirror CMB spectra corresponding to the same model of Mirror Universe.

The first evidence is that, being scaled by the factor x the temperatures in the two sectors, also their temperature fluctuations will be scaled by the same amount, as evident if we look at the lowest ℓ values (the fluctuations seeds are the same for both sectors). Starting from the top-left panel of the figure, we see that the first mirror CMB peak is higher and shifted to higher multipoles than the ordinary one, while other peaks are both lower and at higher ℓ values, with a shift growing with the order of the peak.

⁸Indeed, there is in principle the possibility that mirror CMB photons could influence our CMB photons in case of existence of a photon-mirror photon kinetic mixing [5], but its detection would not be possible with present and probably even future experiments, given the very low estimates for the cross section of this interaction.

⁹Since two worlds have the same microphysics, the life should be possible also in the mirror sector!

Observing all the panels, we understand the effect of a change of the parameter x on the mirror CMB: (i) for lower x -values the first peak is higher (for $x = 0.5$ it is nearly one and half the ordinary one); (ii) the position shifts to much higher multipoles (so that with the same horizontal scale we can no more see some peaks). The reason is that a change of x corresponds to a change of the mirror decoupling time. The mirror photons, which decouple before the ordinary ones, see a smaller sound horizon, scaled approximately by the factor x ; since the first peak occurs at a multipole $\ell \propto (\text{sound horizon})^{-1}$, we expect it to shift to higher ℓ -values by a factor x^{-1} , that is exactly what we observe in the figure.

We have verified that increasing x the mirror CMB is more and more similar to the ordinary one, until for $x = 1$ (not shown in figure) the two power spectra are perfectly coincident (as expected, since in this case the two sectors have exactly the same temperatures, the same particle contents, and then their photons power spectra are necessarily the same).

If we were able to detect both the ordinary and mirror CMB photons, we had two snapshots of the Universe at two different epochs, which were a powerful cosmological instrument, but unfortunately this is impossible, because mirror photons are by definition completely invisible for us.

4 The large scale structure for a Mirror Universe

Given the oscillatory behaviour of the mirror baryons (different from the smooth one of cold dark matter), we expect that MBDM induces specific signatures also on the large scale structure power spectrum.

In order to evaluate this effect, we computed LSS power spectra using the same reference and mirror models used in § 3 for the CMB analysis. The two panels of figure 3 show the LSS for the same models as in figure 1. In order to remove the dependences of units on the Hubble constant, we plot on the x -axis the wave number in units of h and on the y -axis the power spectrum in units of h^3 . The minimum scale (the maximum k) plotted is placed around the limit of the linear regime.

In top panel of the figure we show the dependence on x for different mirror models without CDM; in this case, where all the dark matter is made of mirror baryons, the oscillatory effect is obviously maximum. The first evidence is the strong dependence on x of the beginning of oscillations: it goes to higher scales for higher x , and below $x \simeq 0.3$ the power spectrum for a Mirror Universe approaches more and more the CDM one. This behaviour is a consequence of the x -dependence of the mirror Silk scale, that increases for growing x (for details see Paper I [1] and refs. [10, 11, 20]): this dissipative scale induces a cutoff in the power spectrum, which is damped with an oscillatory behaviour (it will be more evident in figures 4 and 5, where we extend our models to smaller scales within the non linear region). Oscillations begin at the same time of the damping, and they are so deep (because there are many mirror baryons) to go outside the coordinate box. In any case the mirror spectra are always below the ordinary one for every value of x .

The dependence on the amount of mirror baryons is instead shown in the bottom panel of the figure, where only a fraction of the dark matter is made of mirror baryons, while the rest is CDM. Contrary to the CMB case, the matter power spectrum strongly depends on ω'_b . The oscillations are deeper for increasing mirror baryon densities and the spectrum goes more and more away from the pure CDM one. We note also that the damping begins always at the same scale, and thus it depends only on x and not on ω'_b , as we know from the expression of the mirror Silk scale obtained in Paper I [1] and refs. [10, 11, 20]

$$M'_S \sim [f(x)/2]^3 (\omega'_b)^{-5/4} 10^{12} M_\odot, \quad (9)$$

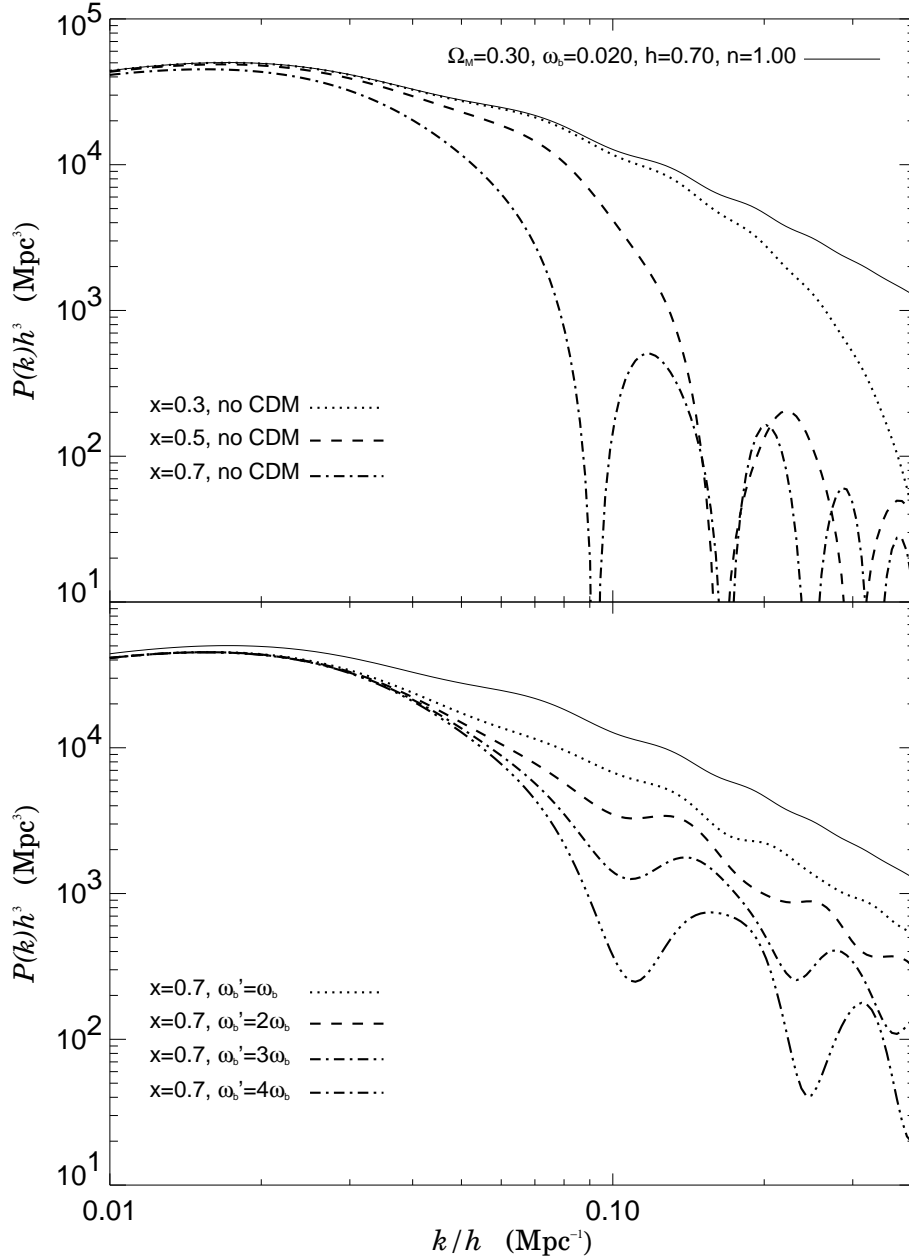


Figure 3: LSS power spectrum in the linear regime for different values of x and $\omega'_b = \Omega'_b h^2$, compared with a standard model (solid line). In order to remove the dependences of units on the Hubble constant, we plot on the x -axis the wave number in units of h and on the y -axis the power spectrum in units of h^3 . *Top panel.* Mirror models with the same parameters as the ordinary one, and with $x = 0.3, 0.5, 0.7$ and $\omega'_b = \Omega_m h^2 - \omega_b$ (no CDM) for all models. *Bottom panel.* Mirror models with the same parameters as the ordinary one, and with $x = 0.7$ and $\omega'_b = \omega_b, 2\omega_b, 3\omega_b, 4\omega_b$.

where $f(x) = x^{5/4}$ for $x > x_{\text{eq}}$ and $f(x) = (x/x_{\text{eq}})^{3/2}x_{\text{eq}}^{5/4}$ for $x < x_{\text{eq}}$.

The same considerations are valid for the oscillation minima, which become much deeper for higher mirror baryon densities, but shift very slightly to lower scales, so that their positions remain practically constant.

4.1 Extension to smaller (non linear) scales

Let us now extend the behaviour of the matter power spectrum to lower scales, which already became non linear. Obviously, since our treatment is based on the linear theory, it is no longer valid in non linear regime. Nevertheless, even if it cannot be used for a comparison with observations, the extension of our models to these scales is very useful to understand the behaviour of the power spectrum in a mirror baryonic dark matter scenario, in particular concerning the position of the cutoff (we recall that its presence could help in avoiding the problem of the CDM scenario with the excessive number of small structures).

Therefore, in figures 4 and 5 we extend the power spectra up to $k/h = 10 \text{ Mpc}^{-1}$ (corresponding to galactic scales), well beyond the limit of the linear regime, given approximately by $k/h < 0.4 \text{ Mpc}^{-1}$.

In figure 4 we plot in both panels the same models as in figure 3. For comparison we show also a standard model characterized by a matter density made almost completely of CDM, with only a small contamination of baryons ($\Omega_b \simeq 0.2\%$ instead of $\simeq 4\%$ of other models). In the top panel, the x -dependence of the mirror power spectra is considered: the vertical scale extends to much lower values compared to figure 3, and we can clearly see the deep oscillations, but in particular it is evident the presence of the previously cited cutoff. For larger values of x oscillations begin earlier and cutoff moves to higher scales. Moreover, note that the model with almost all CDM has more power than the same standard model with baryons, which in turn has more power than all mirror models for any x and for all the scales. In the bottom panel we show the dependence on the mirror baryon content. It is remarkable that all mirror models stop to oscillate at some low scale and then continue with a smooth CDM-like trend. This means that, after the cutoff due to mirror baryons, the dominant behaviour is the one characteristic of cold dark matter models (due to the lack of a cutoff for CDM). Clearly, for higher mirror baryon densities the oscillations continue down to smaller scales, but, contrary to the previous case, where all the dark matter was mirror baryonic, there will always be a scale below which the spectrum is CDM-like.

An interesting point of the mirror baryonic scenario is his capability to mimic a CDM scenario under certain circumstances and for certain measurements. To explain this point, in figure 5 we show models with low x -values (0.2 or 0.1) and all dark matter made of MBDM; we see that for $x = 0.2$ the standard and mirror power spectra are already practically coincident in the linear region. If we go down to $x = 0.1$ the coincidence is extended up to $k/h \sim 1 \text{ Mpc}^{-1}$. In principle, we could still decrease x and lengthen this region of equivalence between the different CDM and MBDM models, but we have to remember that we are dealing with linear models extended to non linear scales, then neglecting all the non linear phenomena (such as merging or stellar feedback), that are very different for the CDM and the MBDM scenarios. In the same plot we also considered a model with $x = 0.2$ and dark matter composed equally by mirror baryons and CDM. This model shows that in principle it's possible a tuning of the cutoff effect reducing the amount of mirror matter, in order to better reproduce the cutoff needed to explain, for example, the low number of small satellites in galaxies.

This work provided for us the linear transfer functions, which constitute the principal

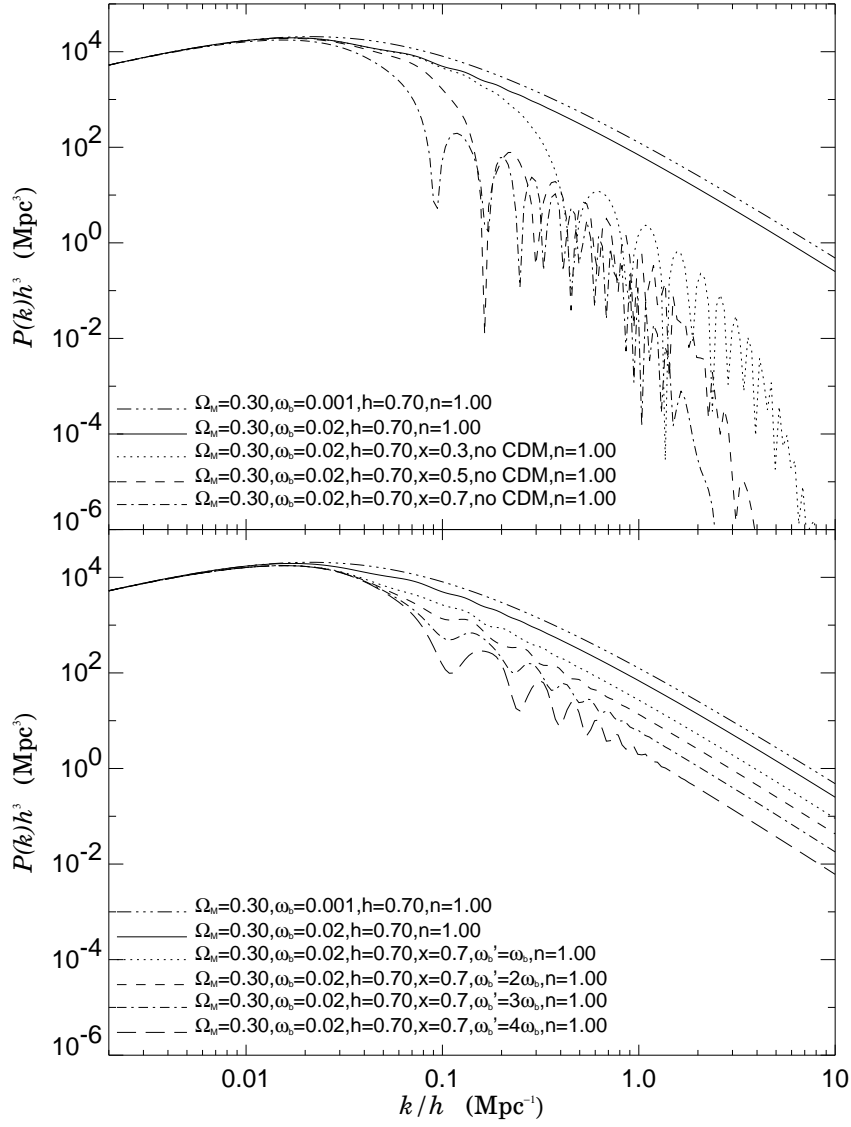


Figure 4: LSS power spectrum beyond the linear regime for different values of x and $\omega'_b = \Omega'_b h^2$, compared with a standard model (solid line). The models have the same parameters as in figure 3. For comparison we also show a standard CDM model with a negligible amount of baryons ($\Omega_b \sim 0.2\%$).

ingredient for the computation of the power spectrum at non linear scales. This calculation is out of the aim of this paper, but could be one of the next steps in the study of the Mirror Universe.

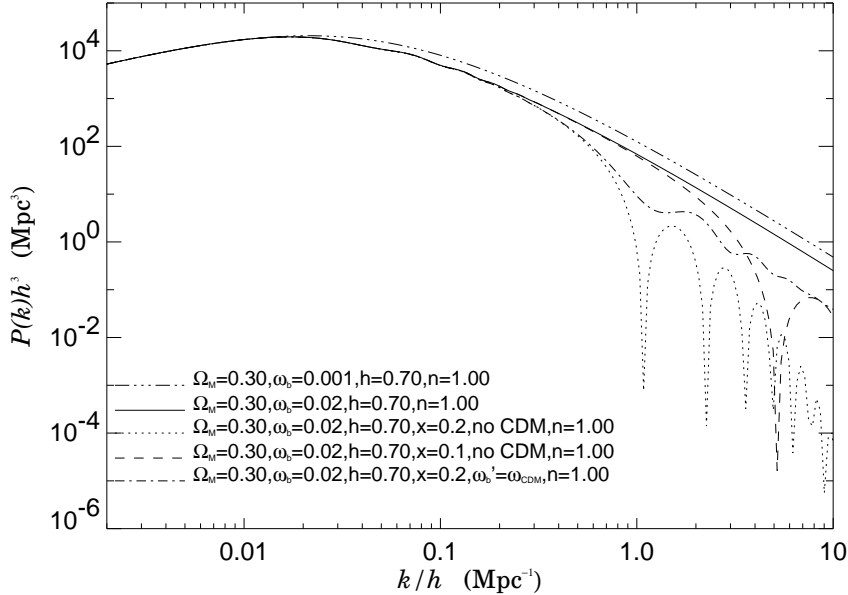


Figure 5: LSS power spectrum beyond the linear regime for two low values of x (0.1 and 0.2) and different amounts of mirror baryons ($\Omega'_b = \Omega_m - \Omega_b$ or $\Omega'_b = \Omega_{CDM}$), compared with a standard model (solid line). The other parameters are the same as in figure 3. For comparison we show also a standard CDM model with a negligible amount of baryons ($\Omega_b \sim 0.2\%$).

5 Dependence on the parameters

The shapes, heights and locations of peaks and oscillations in the photons and matter power spectra are predicted by all models based on the inflationary scenario. Furthermore the details of the features in these power spectra depend critically on the chosen cosmological parameters and on the composition of the Universe, which in turn can be accurately determined by precise measurements of these patterns. In this section we briefly discuss the sensitivity of the C_ℓ 's and $P(k)$'s on the values of some fundamental parameters in a mirror baryonic scenario.

In particular, the exact form of the CMB and LSS power spectra is greatly dependent on assumptions about the matter content of the Universe. Apart from the total density parameter Ω_0 (our models are flat, so Ω_0 is always 1), the composition of the Universe can be parametrized by its components Ω_m and Ω_Λ , and the components of the matter density Ω_b , Ω'_b , Ω_{CDM} . Further parameters are the tilt of scalar fluctuations n , the Hubble parameter h , and the ratio of temperatures in the two sectors x . In addition, we consider also the dependence on the number of massless neutrino species N_ν , in order to compare it with the x -dependence. This is important if we remember that the relativistic mirror particles can be parametrized in terms of effective number of extra-neutrino species (for details see ref. [20]).

Starting from the reference model of parameters $\Omega_m = 0.3$, $\omega_b = \omega'_b = 0.02$, $x = 0.2$, $h = 0.7$ and $n = 1.0$, we change one parameter each time, compute the respective models, and plot the CMB and LSS power spectra in order to show the dependence on it (figures 6 - 13). Then, we compute the relative locations and heights of the first three acoustic

peaks of the CMB angular power spectrum and plot them in figures 14 and 15 in order to compare their sensitivities to the parameters.

In the following we briefly analyze the dependences on every parameter, referring to the figure where the respective models are plotted.

- *Matter density* (fig. 6): Ω_m varies from 0.1 to 0.5. In flat models a decrease in Ω_m implies two things: an increase in Ω_Λ (with the consequent delay in matter-radiation equality) and a decrease in Ω_{CDM} (if we leave unchanged the O and M baryon densities). Both these things correspond to boosting and shifting effects on the acoustic peaks, while the matter power spectrum goes down, given the decreasing of the density of the collisionless species (CDM) and the progressive relative growth of the baryon densities, which are responsible for the oscillatory features.
- *O baryon density* (fig. 7): $\omega_b = \omega'_b$ varies from 0.01 to 0.03. An increase of the baryon fraction increases odd peaks (compression phase of the baryon-photon fluid) due to extra-gravity from baryons with respect to the even peaks (rarefaction phase of the fluid oscillation) in the CMB, and generate deeper oscillations in the LSS. In particular, the relative magnitudes of the first and second acoustic peaks are sensitive to ω_b , as we see also in figure 15. These effects are completely due to O baryons. In fact, even if not shown, we have verified that an increase of ω_b with a constant ω'_b has exactly the same consequences for this value of x , while the effect of M baryons becomes relevant if we raise the temperature of the mirror sector.
- *Hubble constant* (figs. 8 and 9): h varies from 0.50 to 0.90, but now we can leave constant either $\Omega_b = \Omega'_b$ (fig. 8) or $\omega_b = \omega'_b$ (fig. 9). In both cases a decrease in h corresponds to a delay in the epoch of matter-radiation equality and to a different expansion rate. This boosts the CMB peaks and slightly changes their location toward higher ℓ 's (similar to the effect of an increase of Ω_Λ), and induces a decrease in the LSS spectrum. There are slight differences between the two situations of Ω or ω constant, evident in particular on the first acoustic peak and on the matter oscillations. In fact, when we consider $\omega_{b,b'}$ constant, the baryon densities $\Omega_{b,b'} = \omega_{b,b'}/h^2$ grow for decreasing h , then favouring the raise of the first peak in the CMB and the onset of oscillations in the LSS.
- *Spectral index* (fig. 10): n varies from 0.90 to 1.10. Increasing n will raise the power spectra at large ℓ 's with respect to the low ℓ 's and at large values of k with respect to low values. This is not evident in figure (except before the first acoustic peak), where the curves seem nearly parallel as if they were simply vertically shifted; this means a low sensitivity to the spectral index in this range, as also evident in figures 14 and 15 for the CMB.
- *Extra-neutrino species* (fig. 11): ΔN_ν varies from 0.0 to 1.5. The effect of increasing the number of massless neutrino species is a slow raise of the first acoustic peak and a shift to higher ℓ values for next peaks, together with a slight lowering of the matter power spectrum; all these changes are nearly proportional to ΔN_ν , as shown also in figures 14 and 15.
- *Ratio of temperatures* (fig. 12): x varies from 0.2 to 0.7. Concerning the CMB, the effect of raising x is qualitatively the same as an increase in ΔN_ν , but more pronounced (for these “cosmologically compatible” ranges) and with a non-linear dependence. In the LSS spectrum, instead, the situation is different from the case of extra-neutrino species, as now a growth of x induces the onset of the oscillatory

features at lower values of k . These behaviours have been studied in more details in § 3 and § 4.

- *M baryon density* (fig. 13): ω'_b varies from 0.01 ($\omega_b / 2$) to 0.08 ($4\omega_b$). The value of x is now raised to 0.7, because for 0.2 there aren't differences between models with different ω'_b values (we start observing small deviations only for the higher k -values in the matter power spectrum). Also this behaviour has been studied in more details in § 3 and § 4; here we want to emphasize the low sensibility of the CMB on ω'_b (with a slightly stronger dependence starting from the third peak) and, on the contrary, the high sensitivity of the LSS. For the first one, an increase in ω'_b causes a very low increase of the height of the first peak and a progressive more pronounced decrease for the next peaks, while for the second one there is a rapid deepening of the oscillations, slightly changing their locations.

In figures 14 and 15 we focus our attention on the CMB first three peaks, choosing some indicator which could quantify the sensitivity to the parameters previously discussed. In figure 14 we analyze the locations of the peaks, plotting the differences of the locations between the various models and the reference one for the three peaks; in figure 15 we plot the deviations of the differences between the heights of the peaks from the same quantities obtained for the reference model. In this way we obtain a clear picture of the trends of these indicators varying the parameters. These plots provide a useful reference in order to evaluate the influence of each parameter on the CMB and LSS power spectra, and they contain a number of informations; we can extract some of them particularly worth of noting.

Looking at the locations, we see a great sensitivity on the matter density and the Hubble constant, and a negligible one on the spectral index and the amount of mirror baryons. Concerning the extra-neutrino species and the temperature of the sectors, the sensitivities are comparable, but the trends are different: they are respectively a constant slope for ΔN_ν and an increasing one for x .

As regards the peak temperatures, the most sensitive parameter, besides Ω_m and h , is ω_b ; the dependence on n and ω'_b is a bit greater than what it is for the locations, and the differences between the trends with N_ν and x are slightly more evident, specially for values $x > 0.6$.

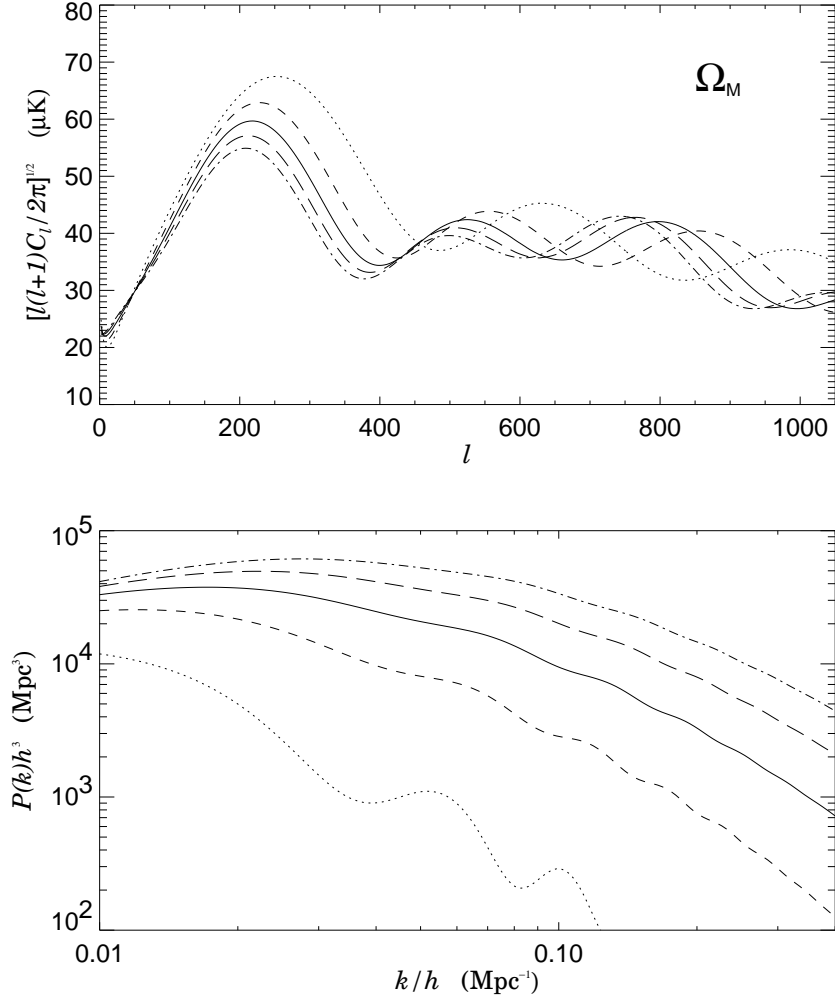


Figure 6: Dependence of the shape of photon and matter power spectra on the matter density Ω_m . The reference model (solid line) has: $\Omega_m = 0.3$, $\omega_b = \omega'_b = 0.02$, $x = 0.2$, $h = 0.7$ and $n = 1.0$. For other models, all the parameters are unchanged except for the one indicated: $\Omega_m = 0.1$ (dot), $\Omega_m = 0.2$ (dash), $\Omega_m = 0.4$ (long dash), $\Omega_m = 0.5$ (dot-dash).

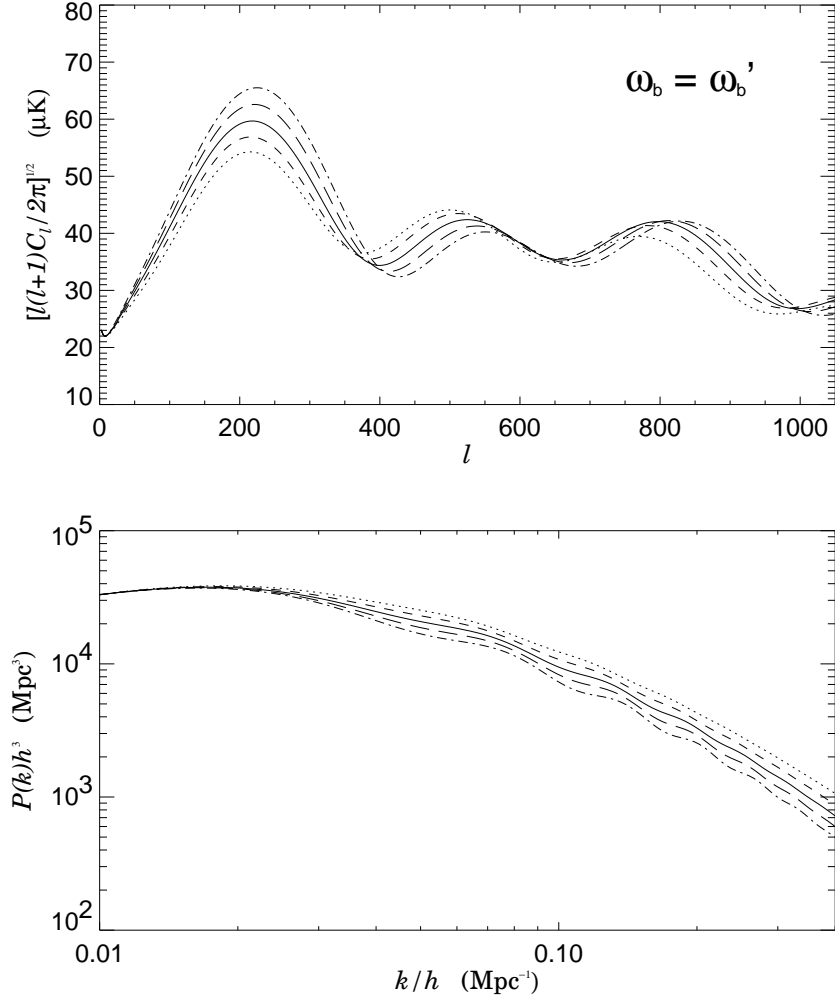


Figure 7: Dependence of the shape of photon and matter power spectra on the ordinary baryon density ω_b with $\omega_b = \omega'_b$. The reference model (solid line) has: $\Omega_m = 0.3$, $\omega_b = \omega'_b = 0.02$, $x = 0.2$, $h = 0.7$ and $n = 1.0$. For other models, all the parameters are unchanged except for the one indicated: $\omega_b = 0.010$ (dot), $\omega_b = 0.015$ (dash), $\omega_b = 0.025$ (long dash), $\omega_b = 0.03$ (dot-dash).

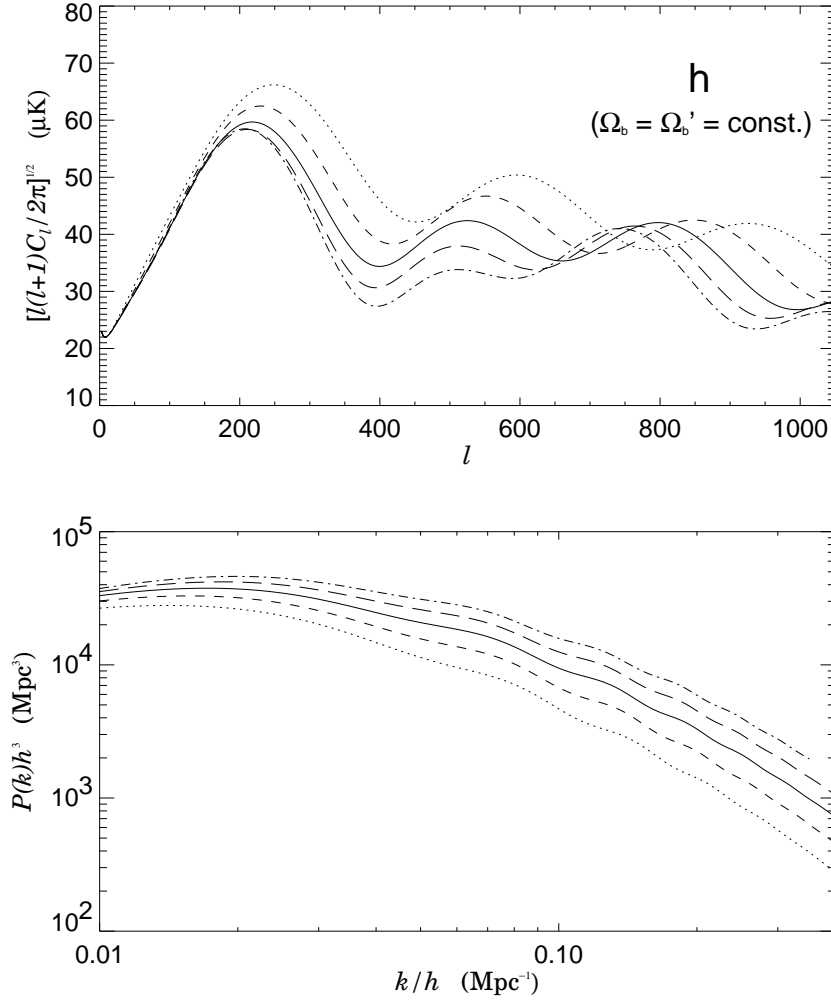


Figure 8: Dependence of the shape of photon and matter power spectra on the Hubble parameter h with $\Omega_b = \Omega'_b = \text{const.}$ The reference model (solid line) has: $\Omega_m = 0.3$, $\Omega_b = \Omega'_b = 0.0408$ (the value obtained for $\omega_b = 0.02$ and $h = 0.7$), $x = 0.2$, $h = 0.7$ and $n = 1.0$. For other models, all the parameters are unchanged except for the one indicated: $h = 0.5$ (dot), $h = 0.6$ (dash), $h = 0.8$ (long dash), $h = 0.9$ (dot-dash).

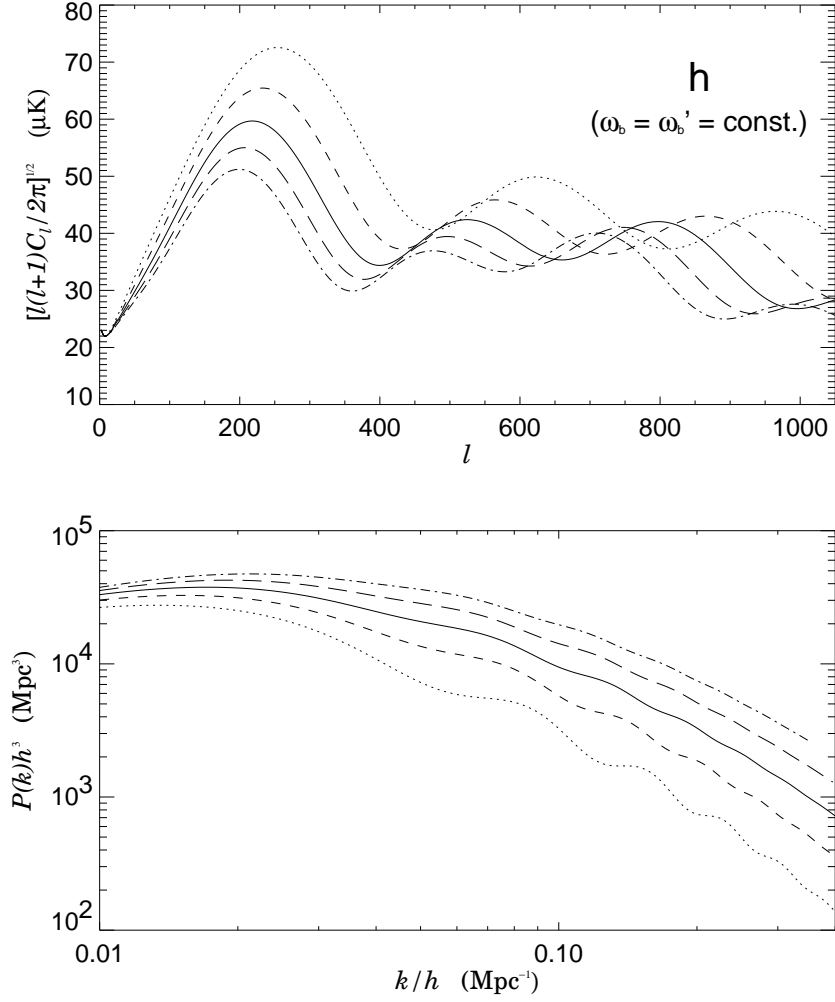


Figure 9: Dependence of the shape of photon and matter power spectra on the Hubble parameter h with $\omega_b = \omega'_b = \text{const.}$ The reference model (solid line) has: $\Omega_m = 0.3$, $\omega_b = \omega'_b = 0.02$, $x = 0.2$, $h = 0.7$ and $n = 1.0$. For other models, all the parameters are unchanged except for the one indicated: $h = 0.5$ (dot line), $h = 0.6$ (dash), $h = 0.8$ (long dash), $h = 0.9$ (dot-dash).

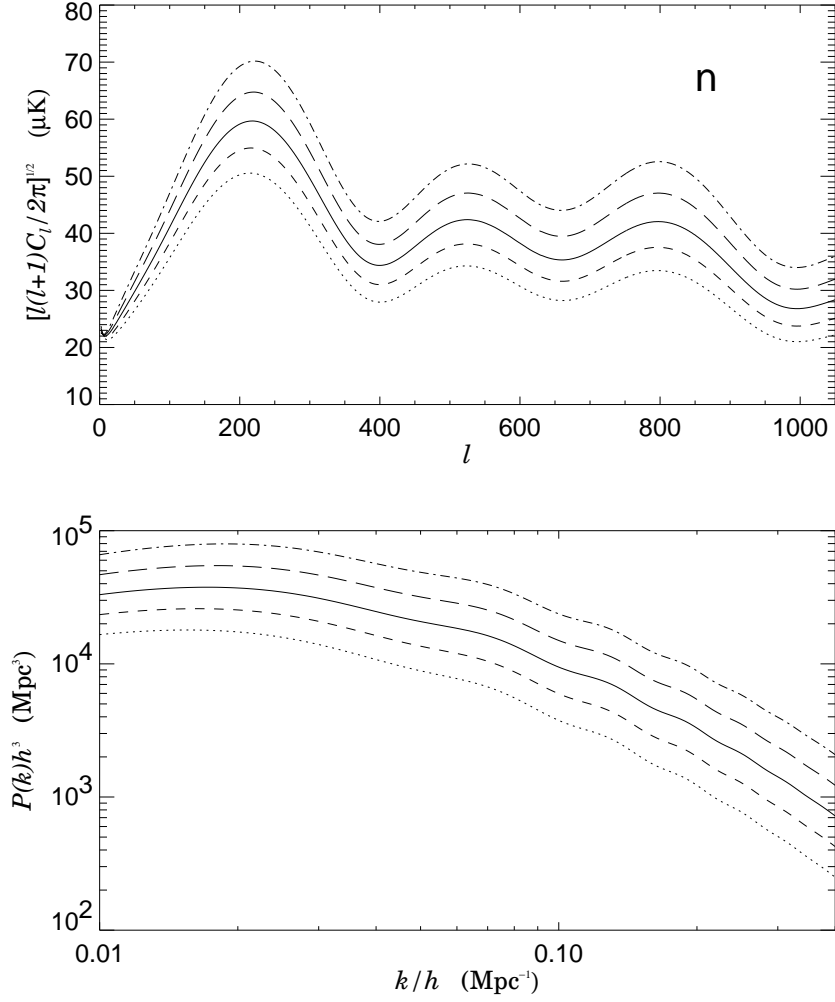


Figure 10: Dependence of the shape of photon and matter power spectra on the scalar spectral index n . The reference model (solid line) has: $\Omega_m = 0.3$, $\omega_b = \omega'_b = 0.02$, $x = 0.2$, $h = 0.7$ and $n = 1.0$. For other models, all the parameters are unchanged except for the one indicated: $n = 0.90$ (dot), $n = 0.95$ (dash), $n = 1.05$ (long dash), $n = 1.10$ (dot-dash).

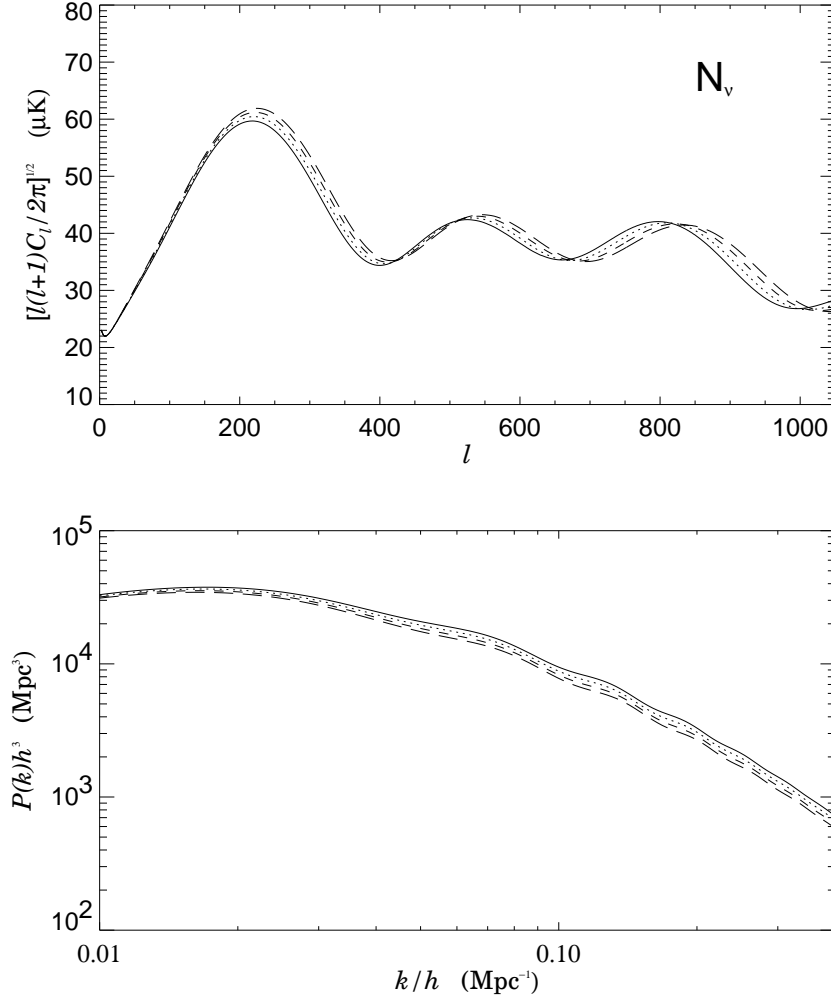


Figure 11: Dependence of the shape of photon and matter power spectra on the number of extra-neutrino species ΔN_ν . The reference model (solid line) has: $\Omega_m = 0.3$, $\omega_b = \omega'_b = 0.02$, $x = 0.2$, $h = 0.7$, $n = 1.0$, and $\Delta N_\nu = 0$. For other models, all the parameters are unchanged except for the one indicated: $\Delta N_\nu = 0.5$ (dot), $\Delta N_\nu = 1.0$ (dash), $\Delta N_\nu = 1.5$ (long dash).

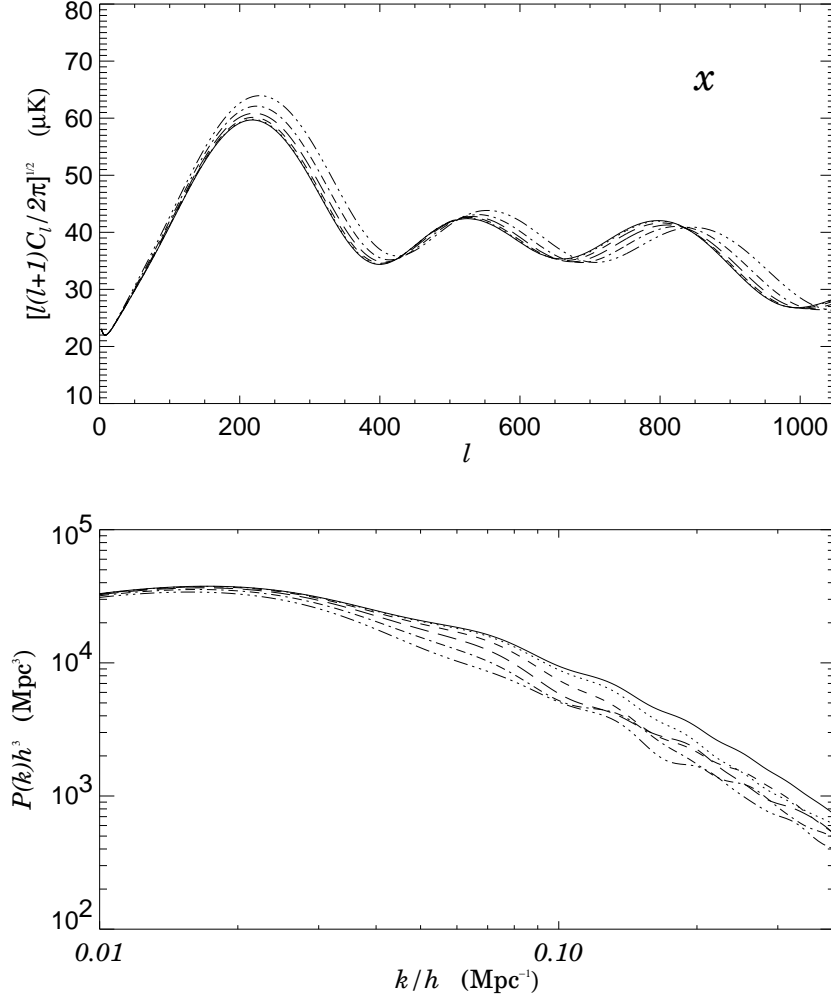


Figure 12: Dependence of the shape of photon and matter power spectra on the ratio of the temperatures of two sectors x . The reference model (solid line) has: $\Omega_m = 0.3$, $\omega_b = \omega'_b = 0.02$, $x = 0.2$, $h = 0.7$ and $n = 1.0$. For other models, all the parameters are unchanged except for the one indicated: $x = 0.3$ (dot), $x = 0.4$ (dash), $x = 0.5$ (long dash), $x = 0.6$ (dot-dash), $x = 0.7$ (dot-dot-dot-dash).

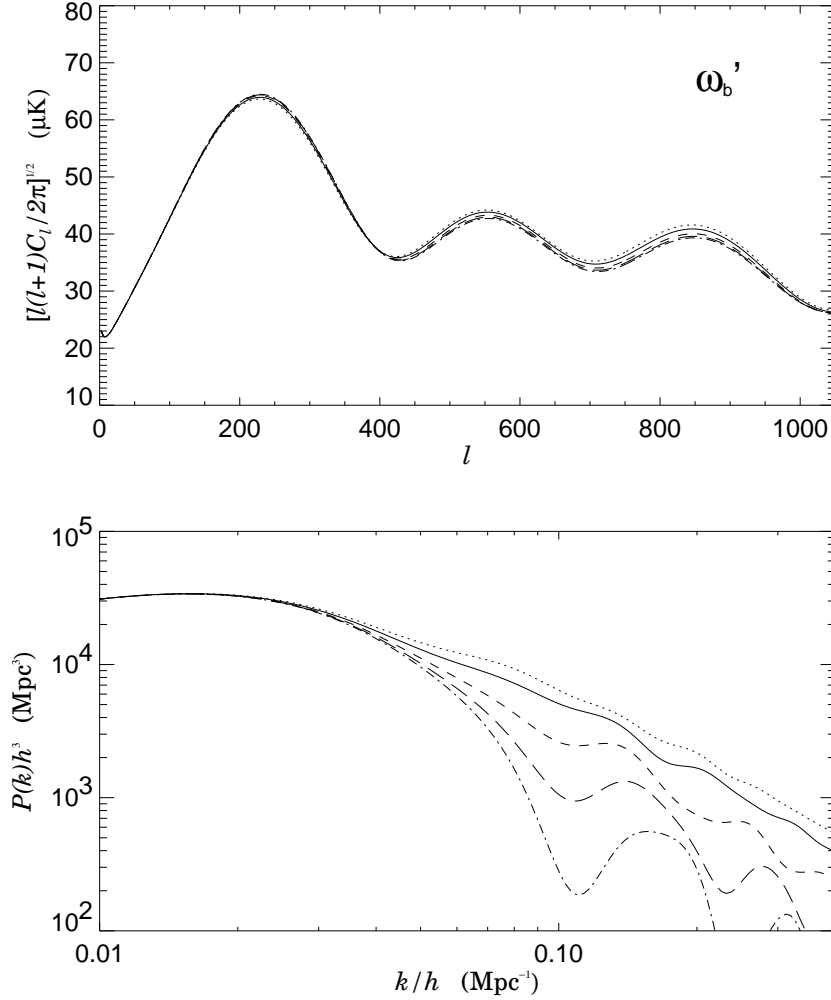


Figure 13: Dependence of the shape of photon and matter power spectra on the mirror baryon density ω'_b keeping constant ω_b . The reference model (solid line) has: $\Omega_m = 0.3$, $\omega_b = \omega'_b = 0.02$, $x = 0.7$ (not 0.2, as previous figures), $h = 0.7$ and $n = 1.0$. For other models, all the parameters are unchanged except for the one indicated: $\omega'_b = 0.01 = \omega_b/2$ (dot), $\omega'_b = 0.04 = 2\omega_b$ (dash), $\omega'_b = 0.06 = 3\omega_b$ (long dash), $\omega'_b = 0.08 = 4\omega_b$ (dot-dash).

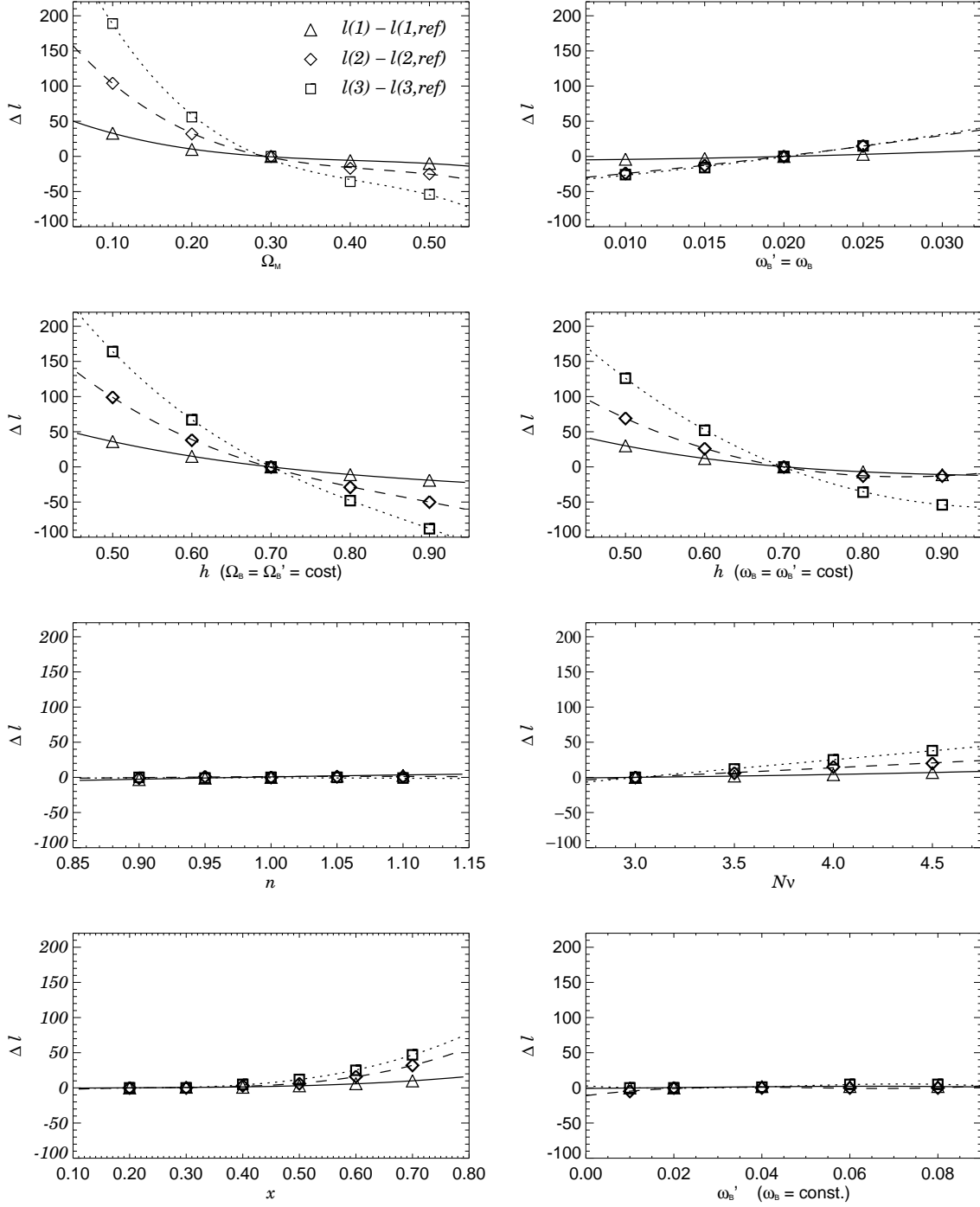


Figure 14: Dependences of the locations of the CMB acoustic peaks on the values of the cosmological parameters: Ω_m , $\omega_b = \omega_b'$, h with $\Omega_b = \Omega_b' = \text{const.}$, h with $\omega_b = \omega_b' = \text{const.}$, n , N_ν , x , and ω_b' with ω_b constant and $x = 0.7$. The three indicators used here are the differences of the positions of the first three peaks of the models from the ones of the reference model. The reference model has: $\Omega_m = 0.3$, $\omega_b = \omega_b' = 0.02$, $x = 0.2$, $h = 0.7$ and $n = 1.0$.

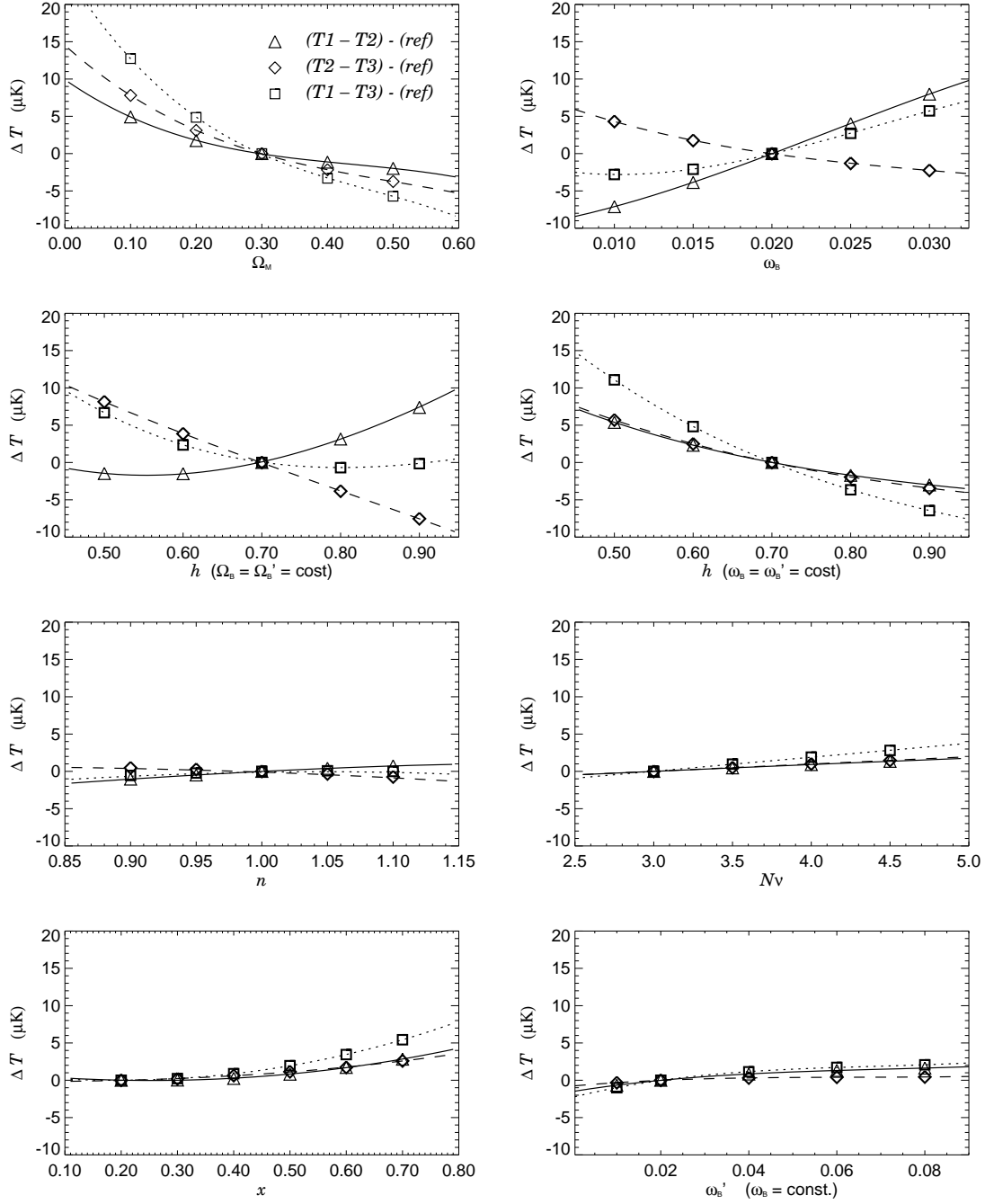


Figure 15: Dependences of the temperatures of the CMB acoustic peaks on the values of the cosmological parameters: Ω_m , $\omega_b = \omega'_b$, h with $\Omega_b = \Omega'_b = \text{const.}$, h with $\omega_b = \omega'_b = \text{const.}$, n , N_ν , x , and ω'_b with ω_b constant and $x = 0.7$. The three indicators used here are the deviations, of the differences between the temperatures of the peaks from the same quantities obtained for a reference model. The reference model has: $\Omega_m = 0.3$, $\omega_b = \omega'_b = 0.02$, $x = 0.2$, $h = 0.7$ and $n = 1.0$.

6 Comparison with observations

So far we have studied the behaviour of the photon and matter power spectra varying many cosmological parameters with special attention to the two mirror parameters, i.e. the ratio of the temperatures of two sectors x and the amount of mirror baryons ω'_b .

Here we want to compare these models with some experimental data, in order to estimate the compatibility of the mirror scenario with observations and possibly reduce the parameter ranges.

As written in § 2, we are not able to fit the parameters now. It is due to the slowness of our present version of the numerical code, but our game will be to choose some representative model and compare it with observations.

In the last decade the anisotropies observed in the CMB temperature became the most important source of information on the cosmological parameters: a lot of experiments (ground-based, balloon and satellite) were dedicated to its measurement. At the same time, many authors proved that its joint analysis with the fluctuations in the matter distribution (they have both the same primordial origin) are a powerful instrument to determine the parameters of the Universe. As in § 3 and § 4, we analyze separately the variation of x and ω'_b in the mirror models, using now both the CMB and LSS informations at the same time.

In order to compare our predictions with observations, we use data among the best ones available at present: for the CMB the WMAP [26] and ACBAR [27] data, and for the LSS the 2dF survey (in particular the binned power spectrum obtained by Tegmark et al. [28]). In order to compare with the standard CDM results, we choose a reference cosmological model with scalar adiabatic perturbations and no massive neutrinos with the following set of parameters [23]: $\Omega_m = 0.25$, $\omega_b = 0.023$, $\Omega_\Lambda = 0.75$, $h = 0.73$, $n = 0.97$. As usually, we include in this model the mirror sector; for the sake of comparison, in all calculations the total amount of matter $\Omega_m = \Omega_{CDM} + \Omega_b + \Omega'_b$ is maintained constant. Mirror baryons contribution is thus always increased at the expenses of diminishing the CDM contribution.

We start from figure 16, where we assume that the dark matter is entirely due to mirror baryons and we consider variations of the x parameter (as in the upper part of figures 1 and 3). In top panel, we see that with the accuracy of the current anisotropy measurements the CMB power spectra for mirror models are perfectly compatible with data, except for the higher- x one. Indeed, the deviations from the standard model are weak for $x \lesssim 0.5$, even in a Universe full of mirror baryons (see § 3). In lower panel, instead, the situation is very different: oscillations due to mirror baryons are too deep to be in agreement with data, and only models with low values of x (namely $x \lesssim 0.3$) are acceptable. Thus, we find the first strong constraint on the mirror parameter space: models with high mirror sector temperatures and all the dark matter made of mirror baryons have to be excluded.

In figure 17 we compare with observations models with the same x , but different mirror baryon contents (as in the bottom panels of figures 1 and 3). The above mentioned low sensitivity of the CMB power spectra on ω'_b doesn't give us indications for this parameter (even for high values of x), but the LSS power spectrum helps us again, confirming a sensitivity to the mirror parameters greater than the CMB one. This is another example of the great advantage of a joint analysis of CMB and LSS power spectra, being the following conclusion impossible looking at the CMB only. This plot tells us that also high values of x can be compatible with observations if we decrease the amount of mirror baryons in the Universe. It is a second useful indication: in case of high mirror sector temperatures we have to change the mirror baryon density in order to reproduce the oscillations present in the LSS data.

Therefore, after the comparison with experimental data, we are left with three possibilities for the Mirror Universe parameters:

- high $x \lesssim 0.5$ and low ω'_b (differences from the CDM in the CMB, and oscillations in the LSS with a depth modulated by the baryon density);
- low $x \lesssim 0.3$ and high ω'_b (completely equivalent to the CDM for the CMB, and few differences for the LSS in the linear region);
- low x and low ω'_b (completely equivalent to the CDM for the CMB, and nearly equivalent for the LSS in the linear region and beyond, according to the mirror baryon density).

Thus, with the current experimental accuracy, we can exclude only models with high x and high ω'_b . Our next step will be to consider some interesting mirror models and compute their power spectra.

In figure 18 we plot models with equal amounts of ordinary and mirror baryons and a large range of temperatures. This is an interesting situation, because the case $\Omega'_b = \Omega_b$ could be favoured in some baryogenesis scenario with some mechanism that naturally lead to equal baryon number densities in both visible and hidden sectors [22]. These models are even more interesting when we consider both their CMB and LSS power spectra. In top panel of figure we see that the temperature anisotropy spectra are fully compatible with observations until $x \simeq 0.5$, without large deviations from the standard case. In bottom panel, we have a similar situation for the matter power spectra, with some oscillations and a slightly greater slope, that could be useful to better fit the oscillations present in the data and to solve the discussed problem of the desired cutoff at low scales. Let us observe that we are deliberately neglecting the biasing problem, given that an indication on its value can come only from a fit of the parameters; then, we have indeed a small freedom to vertically shift the curves in order to better fit the experimental data.

Models of a Mirror Universe where the dark matter is composed in equal parts by CDM and mirror baryons are plotted in figure 19. Here we concentrate on x -values lower than the previous figure, because the greater mirror baryonic density would generate too many oscillations in the linear region of the matter power spectrum. In top panel we show that, apart from little deviations for the model with higher x , all other models are practically the same. In bottom panel, instead, deviations are big, and we can still use LSS as a test for models. Indeed, models with $x \gtrsim 0.4$ are probably to exclude, even taking into account a possible bias. Models with lower x are all consistent with observations.

Observing the figures, even if it is surely premature (given the lack of a detailed statistical analysis of mirror models), we are tempted to guess that mirror baryons could hopefully better reproduce the oscillations present in the LSS power spectra. Thus, we are waiting for more accurate data (in particular for the large scale structure) in order to obtain indications for a standard or a Mirror Universe.

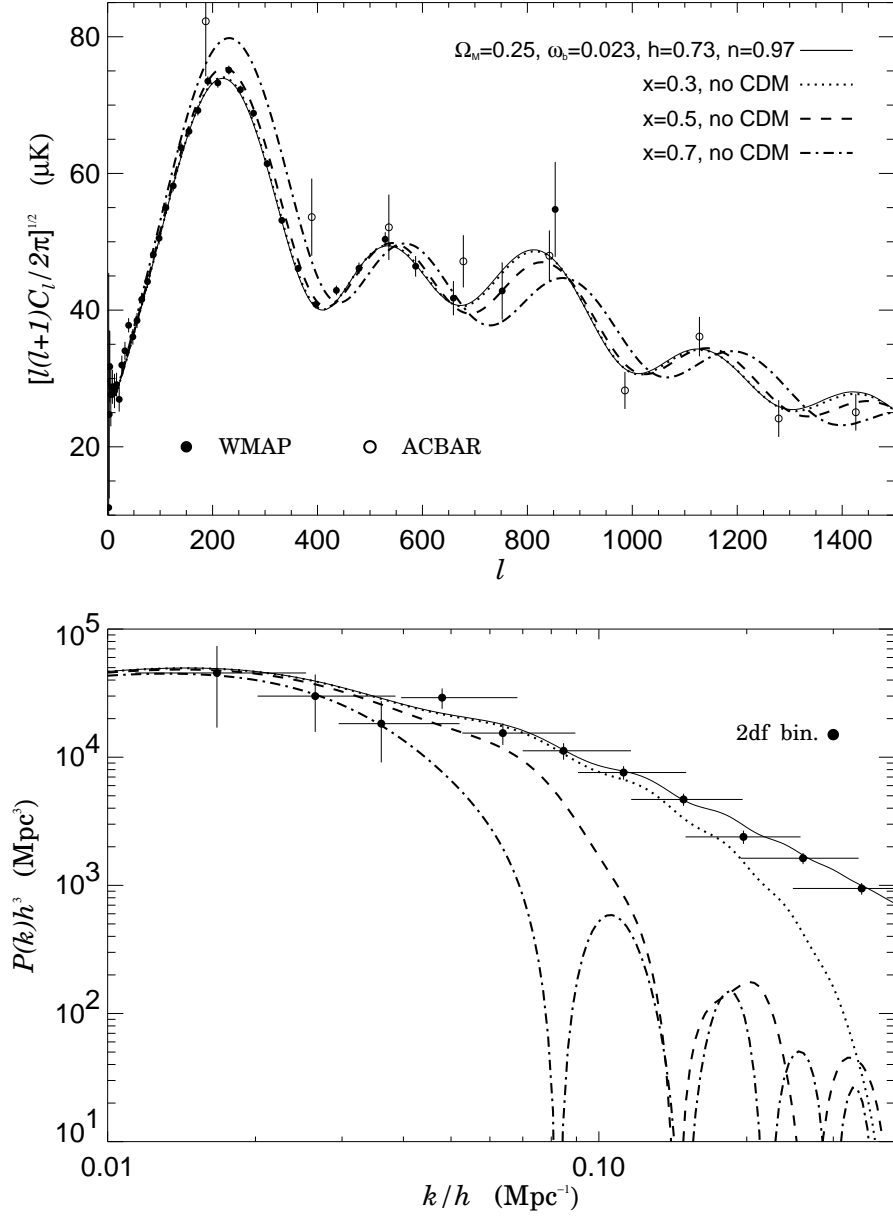


Figure 16: CMB and LSS power spectra for various mirror models with different values of x , compared with observations and with a standard reference model (solid line) of parameters $\Omega_0 = 1$, $\Omega_m = 0.25$, $\Omega_\Lambda = 0.75$, $\omega_b = \Omega_b h^2 = 0.023$, $h = 0.73$, $n = 0.97$. The mirror models have the same parameters as the standard one, but with $x = 0.3, 0.5, 0.7$ and $\omega'_b = \Omega_m h^2 - \omega_b$ (no CDM) for all models. *Top panel.* Comparison of the photon power spectrum with the WMAP and ACBAR data. *Bottom panel.* Comparison of the matter power spectrum with the 2dF binned data.

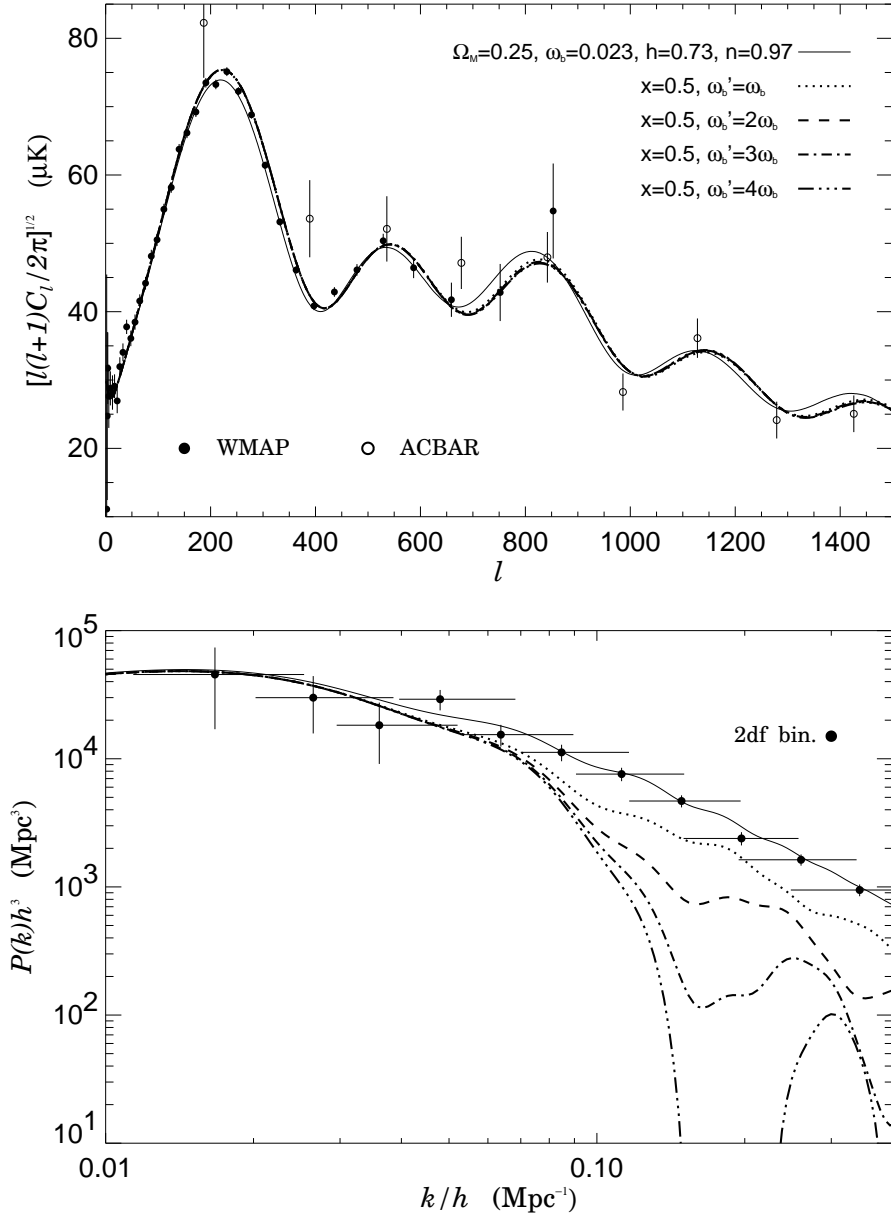


Figure 17: CMB and LSS power spectra for various mirror models with different values of mirror baryon density, compared with observations and with a standard reference model (solid line) of parameters $\Omega_0 = 1, \Omega_m = 0.25, \Omega_\Lambda = 0.75, \omega_b = \Omega_b h^2 = 0.023, h = 0.73, n = 0.97$. The mirror models have the same parameters as the standard one, but with $x = 0.5$ and for $\omega'_b = \omega_b, 2\omega_b, 3\omega_b, 4\omega_b$. *Top panel.* Comparison of the photon power spectrum with the WMAP and ACBAR data. *Bottom panel.* Comparison of the matter power spectrum with the 2dF binned data.

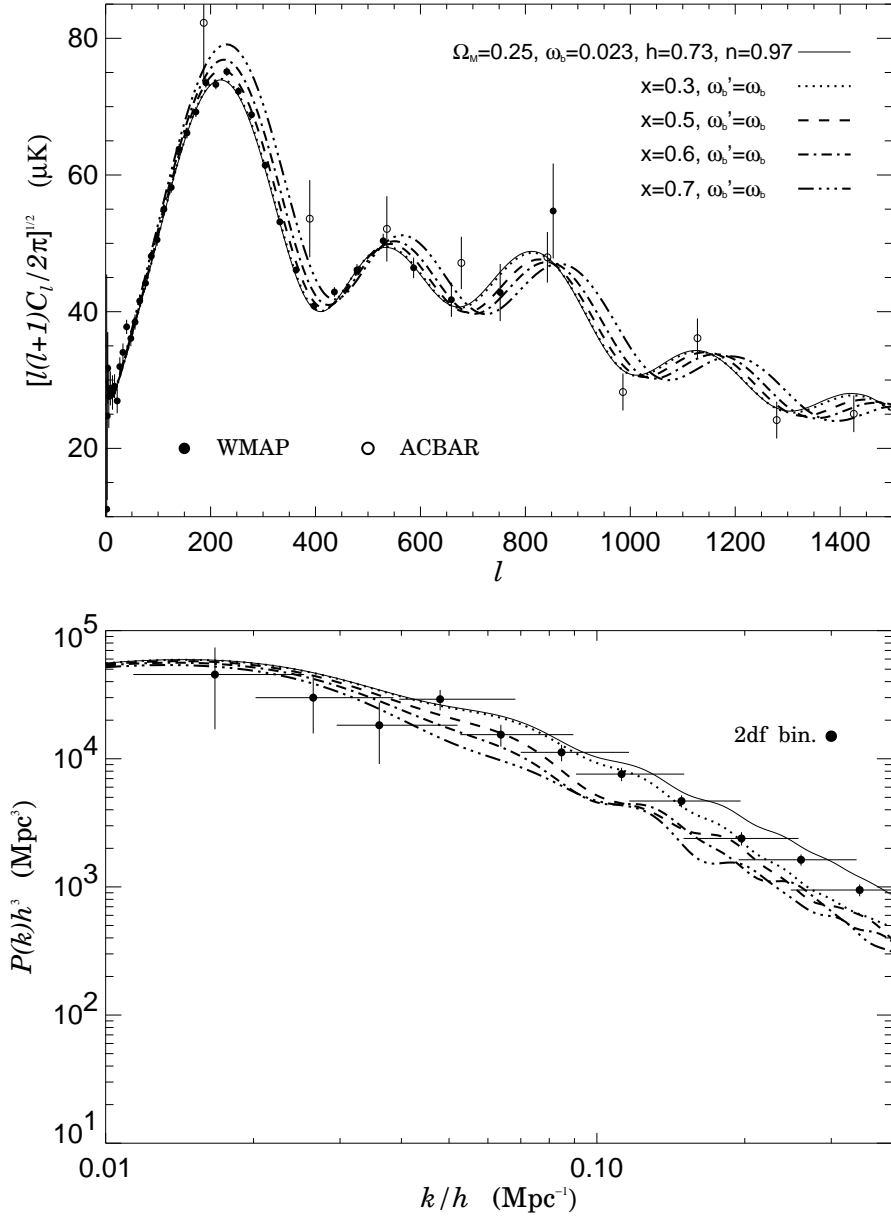


Figure 18: CMB and LSS power spectra for various mirror models with different values of x and equal amounts of ordinary and mirror baryons, compared with observations and with a standard reference model (solid line) of parameters $\Omega_0 = 1, \Omega_m = 0.25, \Omega_\Lambda = 0.75, \omega_b = \Omega_b h^2 = 0.023, h = 0.73, n = 0.97$. The mirror models have the same parameters as the standard one, but with $\omega'_b = \omega_b$ and $x = 0.3, 0.5, 0.6, 0.7$. *Top panel.* Comparison of the photon power spectrum with the WMAP and ACBAR data. *Bottom panel.* Comparison of the matter power spectrum with the 2dF binned data.

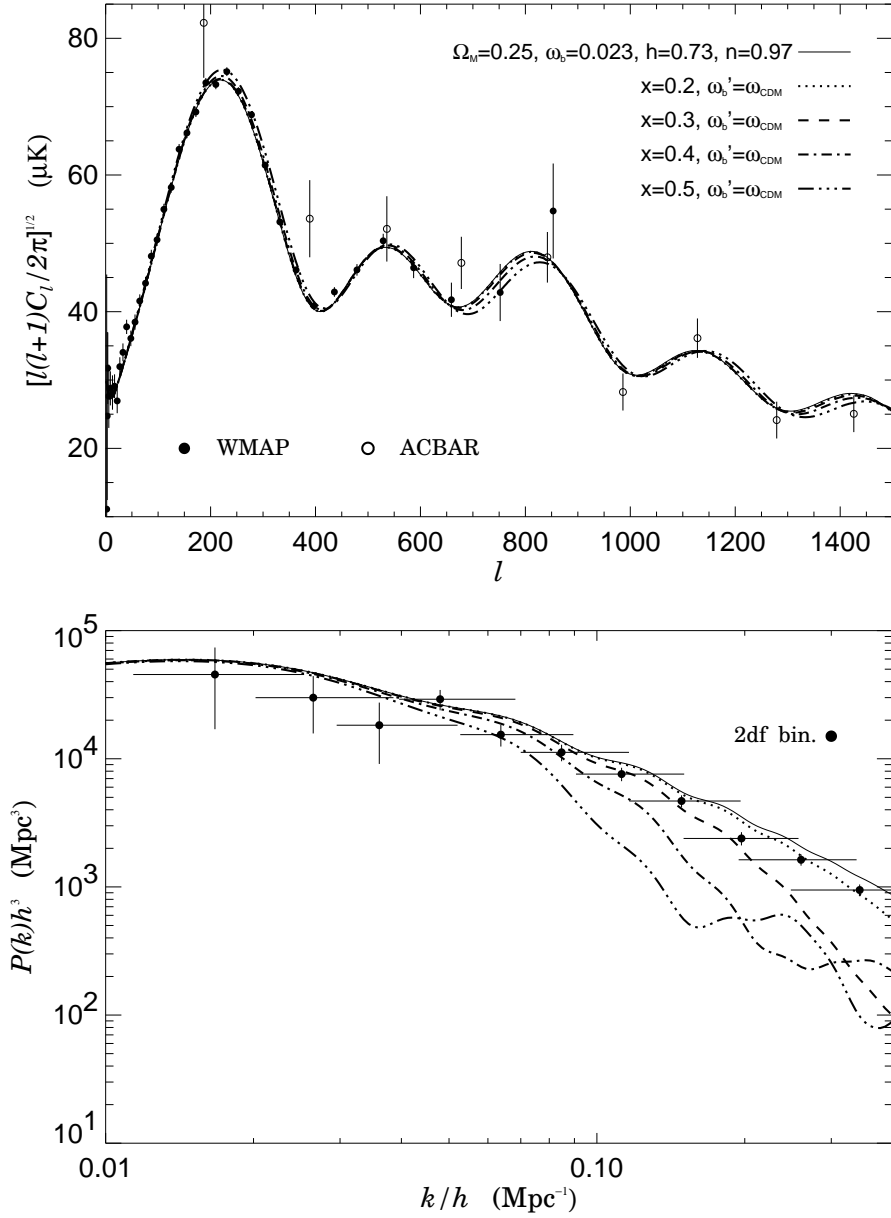


Figure 19: CMB and LSS power spectra for various mirror models with different values of x and equal amounts of CDM and mirror baryons, compared with observations and with a standard reference model (solid line) of parameters $\Omega_0 = 1, \Omega_m = 0.25, \Omega_\Lambda = 0.75, \omega_b = \Omega_b h^2 = 0.023, h = 0.73, n = 0.97$. The mirror models have the same parameters as the standard one, but with $\omega'_b = \omega_{CDM}$ and $x = 0.2, 0.3, 0.4, 0.5$. *Top panel.* Comparison of the photon power spectrum with the WMAP and ACBAR data. *Bottom panel.* Comparison of the matter power spectrum with the 2dF binned data.

7 Conclusions

We have discussed cosmological implications, in terms of cosmic microwave background radiation and large scale structure, of the parallel mirror world with the same microphysics as the ordinary one, but having smaller temperature, $T' < T$, with the limit $T'/T < 0.64$ set by the BBN constraints. This bound implies that the relativistic contribution to the cosmological energy density is dominated by the ordinary sector, while for the matter component the complementary situation can occur and the dark matter of the Universe can be made, in part or entirely, of mirror baryonic dark matter (MBDM).

In the first paper of this series [1] we showed that, since the existence of a mirror hidden sector changes the time of key epochs and the nature of dark matter, there are important consequences in the structure formation scenario for a Mirror Universe. We studied the possible mirror scenarios in presence of adiabatic scalar density perturbations in the context of the Jeans gravitational instability theory, finding important differences from the cold dark matter model.

Here, in order to evaluate the effects of a mirror sector on the CMB and LSS, we modified a numerical code existing for the standard Universe in order to take into account a hidden mirror sector; in this way we were able to predict the expected power spectra of cosmic microwave background and large scale structure for a flat Mirror Universe with adiabatic scalar density perturbations. In this MBDM scenario we studied the dependence of power spectra on mirror parameters x and Ω'_b , and also on other cosmological parameters, as Ω_m , Ω_b , h , n , N_ν . We enlarged our previous studies on this topic [11], considering a much larger set of models. This allowed us to study in detail the sensitivity of mirror CMB and LSS spectra on the cosmological parameters and to show some interesting mirror model which could be a viable alternative to the standard ones.

In CMB spectra we found various differences from a so-called standard (CDM) reference model for $x \gtrsim 0.3$ and a non-linear dependence on x , specially evident in the first and third peaks. The dependence on the mirror baryon density is instead very low. We computed also the power spectrum of mirror CMB photons, even if, unfortunately, by definition we can't reveal them and we cannot exchange the information with the mirror physicists and combine our observations.

Turning to the LSS power spectra, we showed an influence of the mirror sector bigger than for the CMB, with a great dependence on both mirror temperature and baryonic density. Both of them control the oscillations generated in power spectrum, but the first one influences the scale at which they start, while the second one their depth. In this case the mirror sector effects are evident also for low x -values, if we don't take a too small value for Ω'_b . We extended the models also to smaller (non linear) scales, in order to show the cutoff present in the mirror scenario, due to the existence of the dissipative mirror Silk scale. We demonstrated the existence of this cutoff, specially dependent on x -value, but modulated also by Ω'_b . This is an important feature of the mirror structure formation scenario, because it could explain the observed small number of substructures which is a problem for cold dark matter. Furthermore, we showed that for low x -values, $x \lesssim 0.3$, MBDM is equivalent to CDM for the CMB and LSS at linear scales. This is an interesting opportunity for mirror matter, since for low mirror temperatures we could obtain models completely equivalent to the CDM scenario at larger scales (when it works well), but with less power at smaller scales (when it has problems).

In addition, we have shown the dependence of the photon and matter power spectra on the used cosmological parameters, in order to know the relative sensitivities. For the CMB case, we used also some indicators, as the differences between the heights and positions of the peaks compared with the same quantities computed for a reference model.

Our predictions have been compared with the observations (the WMAP [26] and ACBAR [27] data for the CMB, and the 2dF binned data [28] for the LSS) in order to obtain bounds on the possible existence of the mirror sector. In this stage we jointly considered both CMB and LSS data, obtaining important limits on the mirror parameter space. In fact, just from a visual inspection we easily found that mirror models with high x and high Ω'_b are excluded by LSS observations, because they generate too deep oscillations in power spectra.

Even if a statistical analysis is necessary in order to extract detailed informations from the experimental data, nevertheless we can reach some general conclusion in a rather straightforward way:

- The present LSS data are not compatible with a scenario where all the dark matter is made of mirror baryons, unless we consider enough small values of x : $x \lesssim 0.3 \sim x_{\text{eq}}$.
- High values of x , $x > 0.5$, can be excluded even for a relatively small amount of mirror baryons. In fact, we observe relevant effects on LSS and CMB power spectra down to values of M baryon density of the order $\Omega'_b \sim \Omega_b$.
- Intermediate values of x , $0.3 < x < 0.5$, can be allowed if the MBDM is a subdominant component of dark matter, $\Omega'_b \lesssim \Omega_b \lesssim \Omega_{CDM}$.
- For small values of x , $x < 0.3$, the MBDM and the CDM scenarios are indistinguishable as concerns the CMB and the linear LSS power spectra. In this case, in fact, the mirror Jeans and Silk lengths, which mark region of the spectrum where the effects of mirror baryons are visible, decrease to very low values, which undergo non linear growth from relatively large redshift (for details see Paper 1 [1]).

Thus, with the current experimental accuracy, we can exclude only models with high x and high Ω'_b ; however, there can be many possibilities to disentangle the cosmological scenario of two parallel worlds with the future high precision data concerning the large scale structure, CMB anisotropy, structure of the galaxy halos, gravitational microlensing, oscillation of observable particles into their mirror partners, etc.

The aim of these series of papers was contained in a question: “*is mirror matter still a reliable dark matter candidate?*” Now, at the end of this second paper, we reached a partial answer: *on the light of current observations of CMB and LSS at linear scales the mirror baryonic dark matter is fully in agreement with experimental data.* In addition, *we obtained some useful constraints on the mirror parameter space*, that can address our future efforts to understand other aspects of the Mirror Universe. Furthermore, so far the mirror dark matter candidate still shows interesting potentialities to solve some open problems of the “standard” cosmological scenario.

Acknowledgements

I am grateful to my invaluable collaborators Zurab Berezhiani, Denis Comelli and Francesco Villante. I would like to thank also Silvio Bonometto, Stefano Borgani, Alfonso Cavaliere and Nicola Vittorio for interesting discussions.

References

- [1] P. Ciarcelluti, astro-ph/0409630.

- [2] Z. Berezhiani, Acta Phys. Polon. B 27 (1996) 1503;
 R. Foot, H. Lew and R. R. Volkas, JHEP 007, 032 (2000) [hep-ph/0006027];
 R. N. Mohapatra, S. Nussinov and V. L. Teplitz, Phys. Rev. D 66, 063002 (2002) [hep-ph/0111381].
- [3] R. Foot, H. Lew and R. R. Volkas, Phys. Lett. B 272, 67 (1991).
 The idea of mirror particles was earlier discussed in:
 T. D. Lee and C. N. Yang, Phys. Rev. 104, 256 (1956);
 I. Kobzarev, L. Okun and I. Pomeranchuk, Sov. J. Nucl. Phys. 3, 837 (1966);
 M. Pavsic, Int. J. Theor. Phys. 9, 229 (1974).
 For a review:
 R. Foot, hep-ph/0207175;
 R. Foot, *Shadowlands, quest for mirror matter in the Universe*, Universal Publishers, Parkland FL, 2002;
 R. Foot, astro-ph/0407623;
 Z. Berezhiani, Int. J. Mod. Phys. A 19, 3775 (2004) [hep-ph/0312335].
- [4] S. I. Blinnikov and M. Yu. Khlopov, Sov. J. Nucl. Phys. 36, 472 (1982);
 S. I. Blinnikov and M. Yu. Khlopov, Sov. Astron. 27, 371 (1983).
- [5] B. Holdom, Phys. Lett. B 166, 196 (1986);
 E. Carlson and S. Glashow, Phys. Lett. B193, 168 (1987);
 R. Foot and X-G. He, Phys. Lett. B 267, 509 (1991);
 M. Collie and R. Foot, Phys. Lett. B 432, 134 (1998) [hep-ph/9803261];
 A. Yu. Ignatiev and R. R. Volkas, Phys. Lett. B 487, 294 (2000) [hep-ph/0005238];
 R. Foot, A. Yu. Ignatiev and R. R. Volkas, Phys. Lett. B 503, 355 (2001) [astro-ph/0011156].
- [6] E. Akhmedov, Z. Berezhiani and G. Senjanović, Phys. Rev. Lett. 69, 3013 (1992);
 R. Foot, Mod. Phys. Lett. A 9, 169 (1994) [hep-ph/9402241];
 R. Foot and R. R. Volkas, Phys. Rev. D 52, 6595 (1995) [hep-ph/9505359];
 Z. Berezhiani, R.N. Mohapatra, Phys. Rev. D 52, 6607 (1995) [hep-ph/9505385];
 Z. Silagadze, Phys. Atom. Nucl. 60, 272 (1997) [hep-ph/9503481];
 R. Foot, R.R. Volkas, Phys. Rev. D 61, 043507 (2000) [hep-ph/9904336];
 V. Berezhinsky, M. Narayan, F. Vissani, Nucl. Phys. B 658, 254 (2003) [hep-ph/0210204].
- [7] S. Blinnikov, astro-ph/9801015;
 R. Foot, Phys. Lett. B 452, 83 (1999) [astro-ph/9902065];
 R.N. Mohapatra, V. Teplitz, Phys. Lett. B 462, 302 (1999) [astro-ph/9902085].
- [8] S. Blinnikov, astro-ph/9902305;
 R. Volkas, Y. Wong, Astropart. Phys. 13, 21 (2000) [astro-ph/9907161];
 R.N. Mohapatra, S. Nussinov and V.L. Teplitz, Astropart. Phys. 13, 295 (2000) [astro-ph/9909376];
 S. Blinnikov, Surveys High Energ. Phys. 15, 37 (2000) [astro-ph/9911138];
 R. Foot and Z. K. Silagadze, astro-ph/0404515.
- [9] Z. Berezhiani, Phys. Lett. B 417, 287 (1998) [hep-ph/9609342];
 Z. Berezhiani, L. Gianfagna and M. Giannotti, Phys. Lett. B 500, 286 (2001) [hep-ph/0009290];
 L. Gianfagna, M. Giannotti and F. Nesti, hep-ph/0409185.

- [10] A. Yu. Ignatiev and R. R. Volkas, Phys. Rev. D 68, 023518 (2003) [hep-ph/0304260].
- [11] Z. Berezhiani, P. Ciarcelluti, D. Comelli and F. L. Villante, astro-ph/0312605;
P. Ciarcelluti, astro-ph/0312607;
P. Ciarcelluti, astro-ph/0409629.
- [12] R.N. Mohapatra, V. Teplitz, Astrophys. J. 478, 29 (1997) [astro-ph/9603049];
R.N. Mohapatra, V. Teplitz, Phys. Rev. D 62, 063506 (2000) [astro-ph/0001362];
R. Foot and R. R. Volkas, astro-ph/0407522.
- [13] S. L. Glashow, Phys. Lett. B 167, 35 (1986);
R. Foot and S. N. Gninenko, Phys. Lett. B 480, 171 (2000) [hep-ph/0003278];
R. Foot, astro-ph/0309330;
S.N. Gninenko, Phys. Lett. B 326 (1994) 317.
- [14] A. Badertscher *et al.*, hep-ex/0311031.
- [15] R. Foot, Phys. Rev. D 69, 036001 (2004) [hep-ph/0308254];
R. Foot, astro-ph/0403043;
R. Foot, Mod. Phys. Lett. A 19, 1841 (2004) [astro-ph/0405362].
- [16] A. Yu. Ignatiev and R. R. Volkas, Phys. Rev. D 62, 023508 (2000) [hep-ph/0005125];
Z. K. Silagadze, Acta Phys. Pol. B 32, 99 (2001) [hep-ph/0002255];
R. Foot, Acta Phys. Polon. B 32, 3133 (2001) [hep-ph/0107132];
R. Foot and T. L. Yoon, Acta Phys. Polon. 33, 1979 (2002) [astro-ph/0203152];
R. Foot and S. Mitra, Astropart. Phys. 19, 739 (2003) [astro-ph/0211067];
A. Yu. Ignatiev and R. R. Volkas, hep-ph/0306120;
R. Foot and S. Mitra, Phys. Rev. D 68, 071901 (2003) [hep-ph/0306228];
Z. K. Silagadze, astro-ph/0311337.
- [17] S. Mitra and R. Foot, Phys. Lett. B 558, 9 (2003) [astro-ph/0301229];
R. Foot and S. Mitra, Phys. Lett. A 315, 178 (2003) [cond-mat/0306561].
- [18] R. Foot and R. R. Volkas, Phys. Lett. B 517, 13 (2001) [hep-ph/0108051].
- [19] R. Foot, Phys. Lett. B 471, 191 (1999) [astro-ph/9908276];
R. Foot, Phys. Lett. B 505, 1 (2001) [astro-ph/0101055];
R. Foot and Z. K. Silagadze, Acta Phys. Pol. B 32, 2271 (2001) [astro-ph/0104251];
R. Foot, A. Yu. Ignatiev and R. R. Volkas, Astropart. Phys. 17, 195 (2002) [astro-ph/0010502];
Z. K. Silagadze, Acta Phys. Pol. B 33, 1325 (2002) [astro-ph/0110161];
R. Foot, astro-ph/0406257.
- [20] Z. Berezhiani, D. Comelli and F. L. Villante, Phys. Lett. B 503, 362 (2001) [hep-ph/0008105].
- [21] E. W. Kolb, D. Seckel and M. S. Turner, Nature 314, 415 (1985);
H. M. Hodges, Phys. Rev. D 47, 456 (1993);
Z. G. Berezhiani, A. D. Dolgov and R. N. Mohapatra, Phys. Lett. B 375, 26 (1996) [hep-ph/9511221];
V. Berezhinsky and A. Vilenkin, Phys. Rev. D 62, 083512 (2000) [hep-ph/9908257].
- [22] L. Bento and Z. Berezhiani, Phys. Rev. Lett. 87, 231304 (2001) [hep-ph/0107281];
L. Bento and Z. Berezhiani, hep-ph/0111116;

- L. Bento and Z. Berezhiani, *Fortsch. Phys.* 50 (2002) 489;
R. Foot and R. R. Volkas, *Phys. Rev. D* 68, 021304 (2003) [hep-ph/0304261];
R. Foot and R. R. Volkas, *Phys. Rev. D* 69, 123510 (2004) [hep-ph/0402267].
- [23] D.N. Spergel *et al.*, *Astrophys. J. Suppl.* 148, 175 (2003) (astro-ph/0302209).
- [24] C. Ma & E. Bertschinger, *Astrophys. J.* 455, 7 (1995) [astro-ph/9506072].
- [25] E.F. Bunn & M. White, *Astrophys. J.* **480**, 6 (1997) [astro-ph/9607060].
- [26] G. Hinshaw *et al.*, *Astrophys. J. Suppl.* 148 (2003) 135 [astro-ph/0302217].
- [27] C.L. Kuo *et al.*, *Astrophys. J.* 600, 32 (2004) [astro-ph/0212289].
- [28] M. Tegmark, A.J.S. Hamilton, Y. Xu, *MNRAS* 335 (2002) 887 [astro-ph/0111575].